MESS - Mass loss of Evolved StarS
An overview

Martin Groenewegen
martin.groenewegen@oma.be

on behalf of the MESS consortium

Herschel - Planck launch 14 May 2009

3.3m effective diameter

3 year of Routine Phase starting Dec. 2009

EoHe: 29 April 2013

Herschel instruments

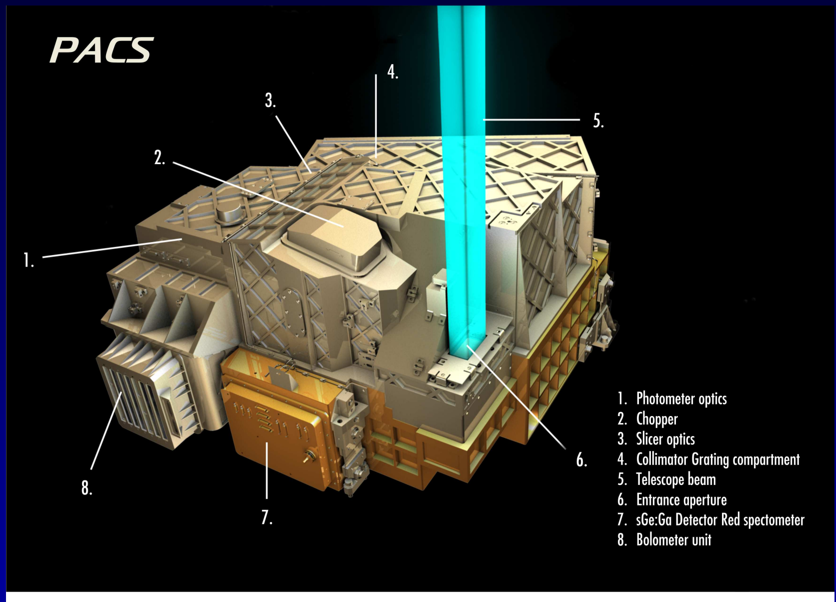

PACS - SPIRE - HIFI

FWHM:

5.6, 6.8, 11.4″ (PACS) (70, 100, 160μm)

18.1, 25.2, 36.6″ (SPIRE) (250, 350, 500 μm)

Evolved stars

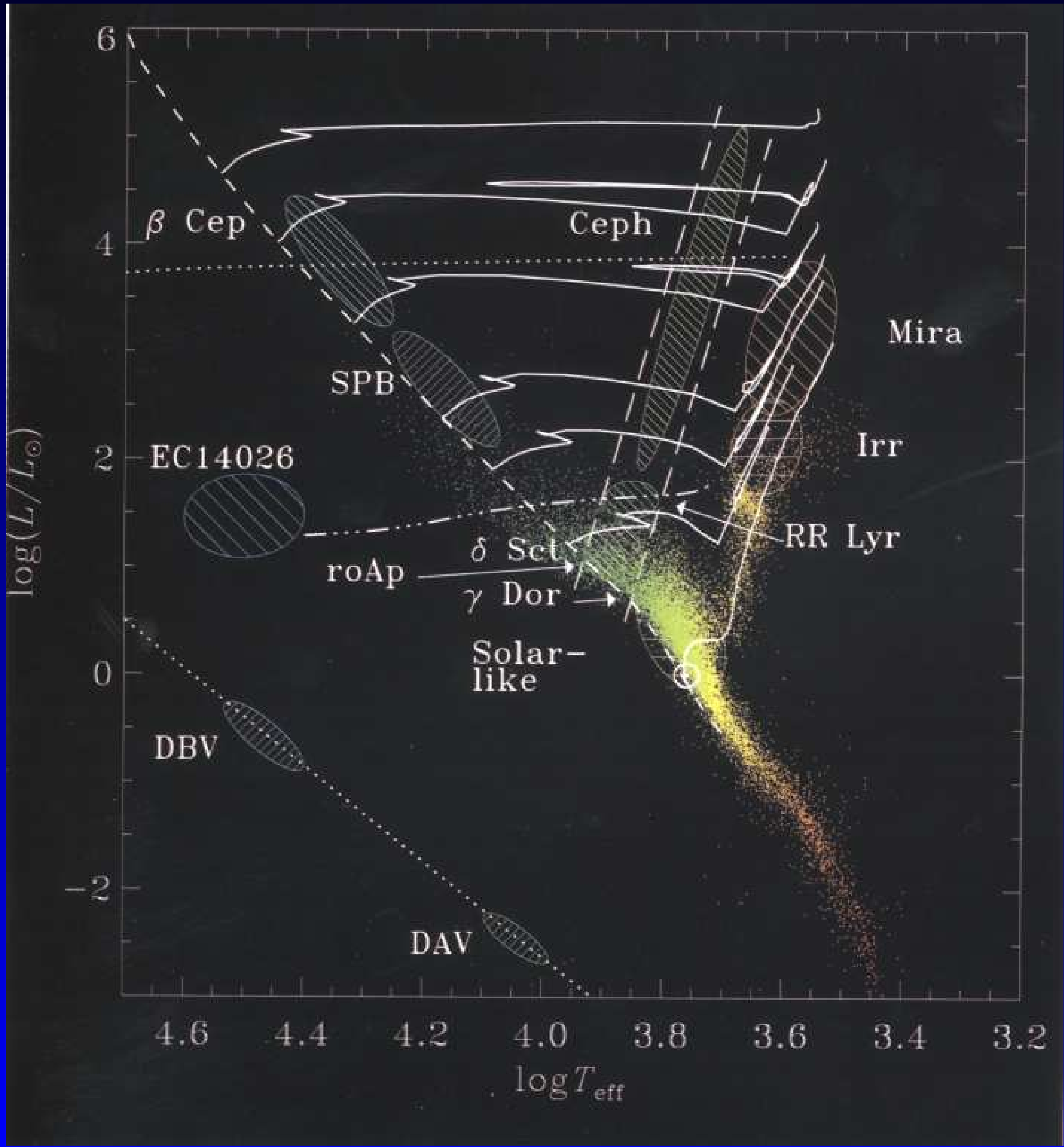

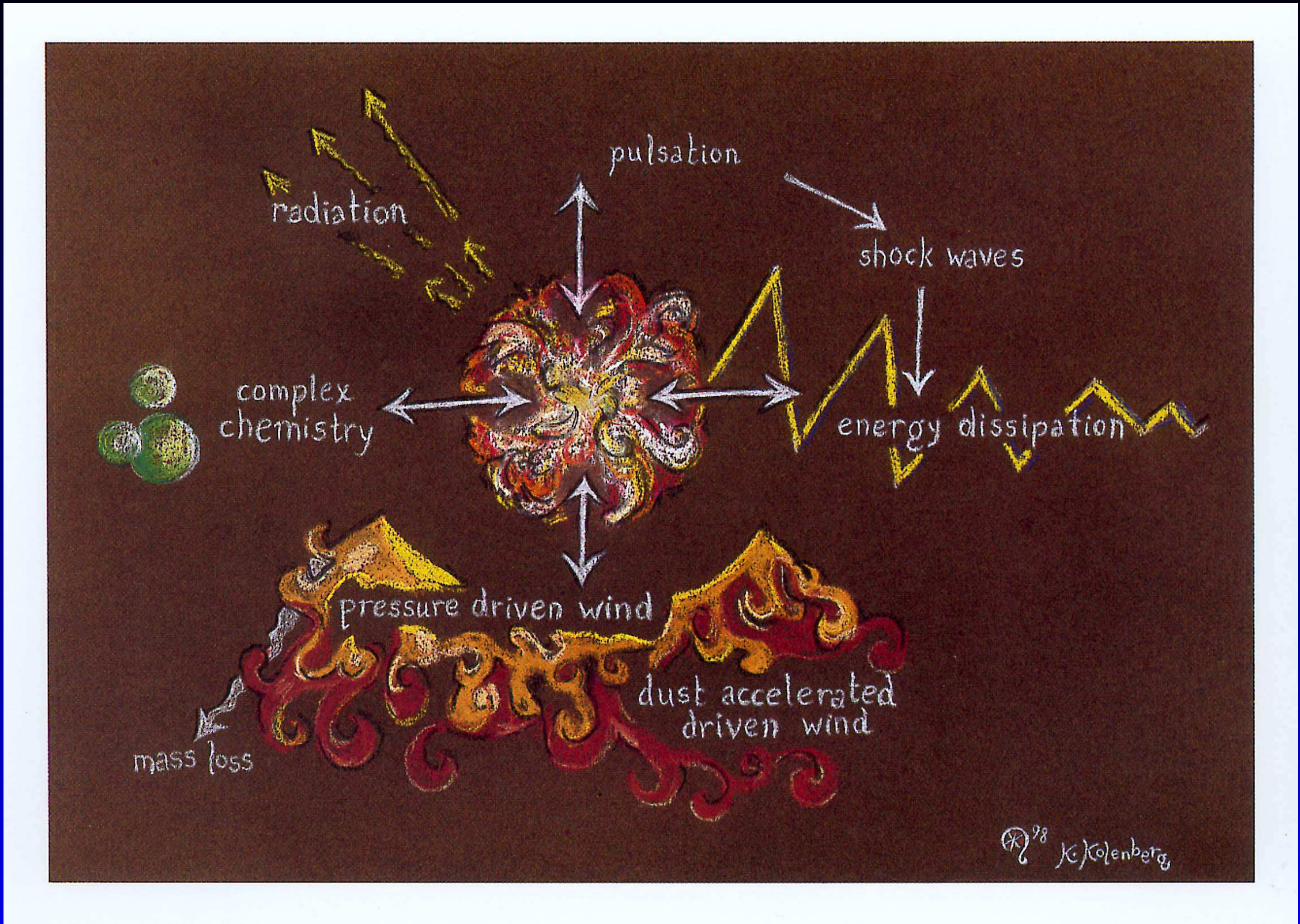
radiation
pulsation
shock waves
complex
chemistry
energy dissipation
pressure driven wind
dust accelerated
driven wind
mass loss
'98 K. Kolenberg

Lifecycle of dust and gas

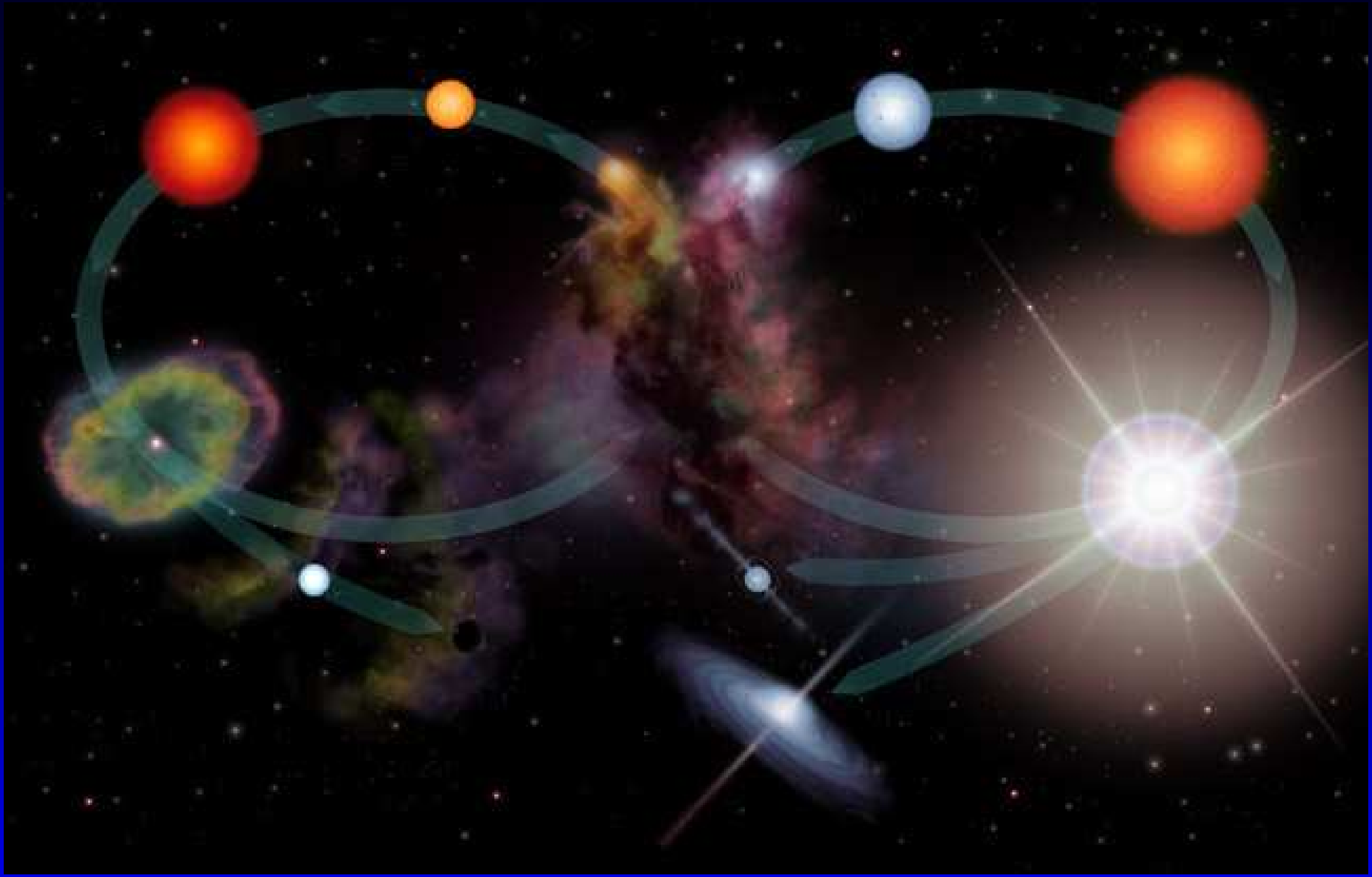

http://hea-www.cfa.harvard.edu/CHAMP/EDUCATION/PUBLIC/starlifecycles_pics.html

Evolved stars GT Key Programs

- MESS (Mass loss of Evolved StarS)
PACS + SPIRE
(PI: Martin Groenewegen
PACS Co-PI:Christoffel Waelkens,KUL,IMEC,CSL)

PACS (50-200 μm) SPIRE (200-650 μm)

both have a bolometer array (FOV of a few arcmin)

both have a spectrometer (R= 1000-2000)

- HIFISTARS - HIFI (PI: Valentin Bujarrabal)

- Other smaller programs in GT2, OT1, OT2

MESS

This GT KP aims at studying the circumstellar matter in evolved objects

- AGB, Post-AGB, PNe, RSG, WR, LBV, SN
    - Photometric mapping of nearby objects
    - Spectroscopy of nearby objects
    - SPIRE and PACS
- Mass-loss dominates the evolution
  How? How much? Time evolution? Spherical?
  Production of dust
- $\dot{M}(Z)$
  AGB vs. SN gas & dust return at high-z

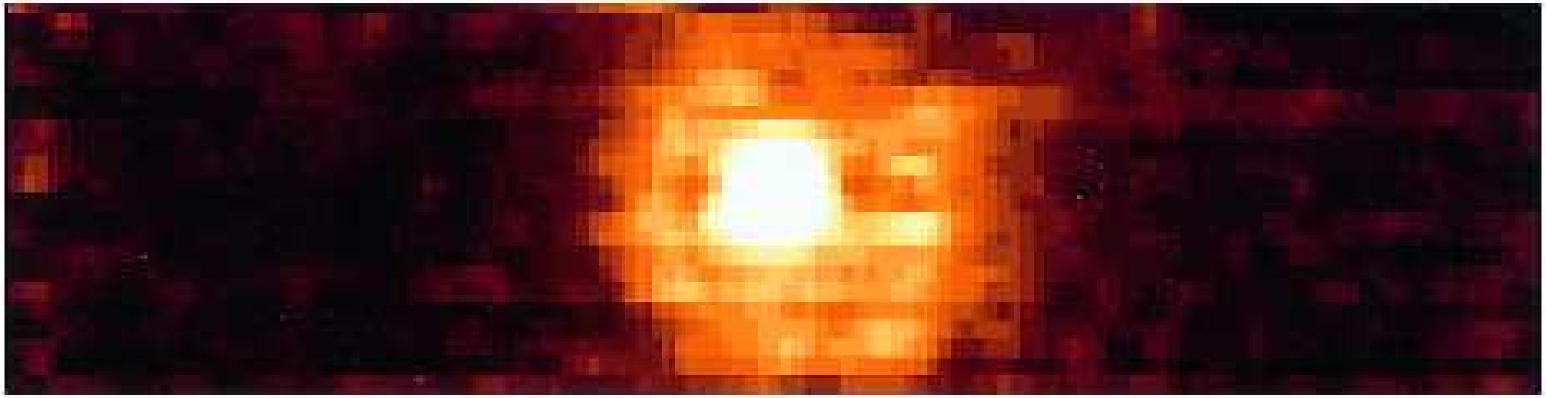

Fig. 1. 90 μm image of Y CVn taken with PHT-C100 array detector and C90 filter displayed in linear brightness scale.

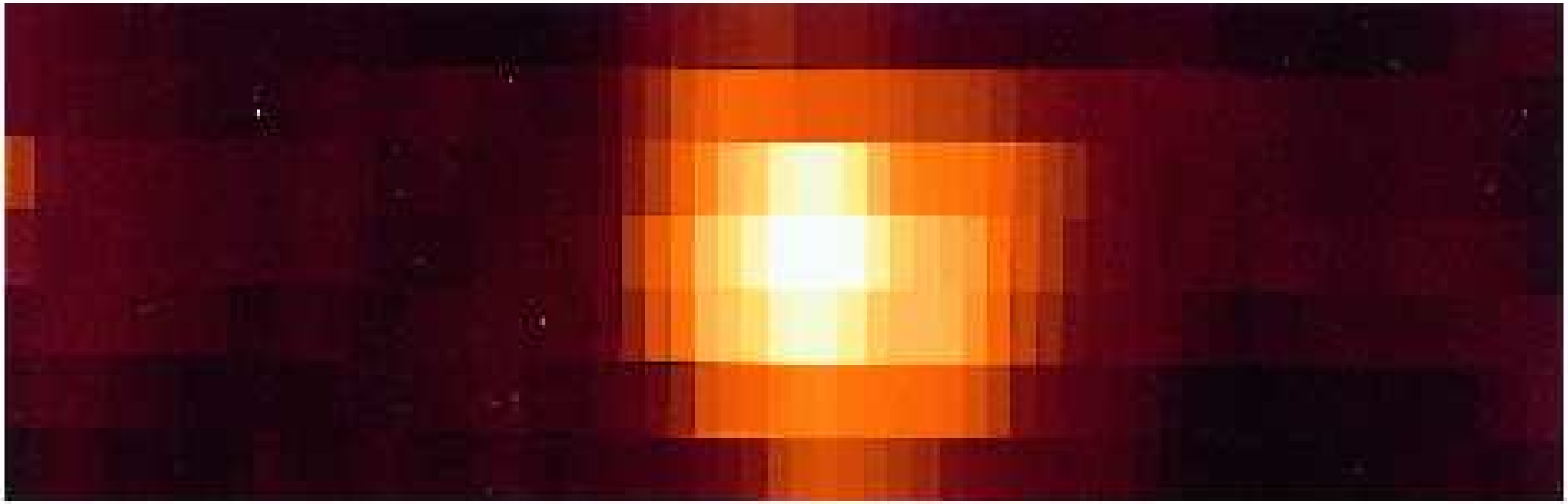

Fig. 2. 160 μm image of Y CVn taken with PHT-C200 array detector and C160 filter displayed in linear brightness scale.

Y CVn

Izumiura et al. (1996), $8' \times 35'$ ISOPHOT map

Spectroscopy of nearby objects

Goal: Study of
dust properties, molecular lines, emission lines

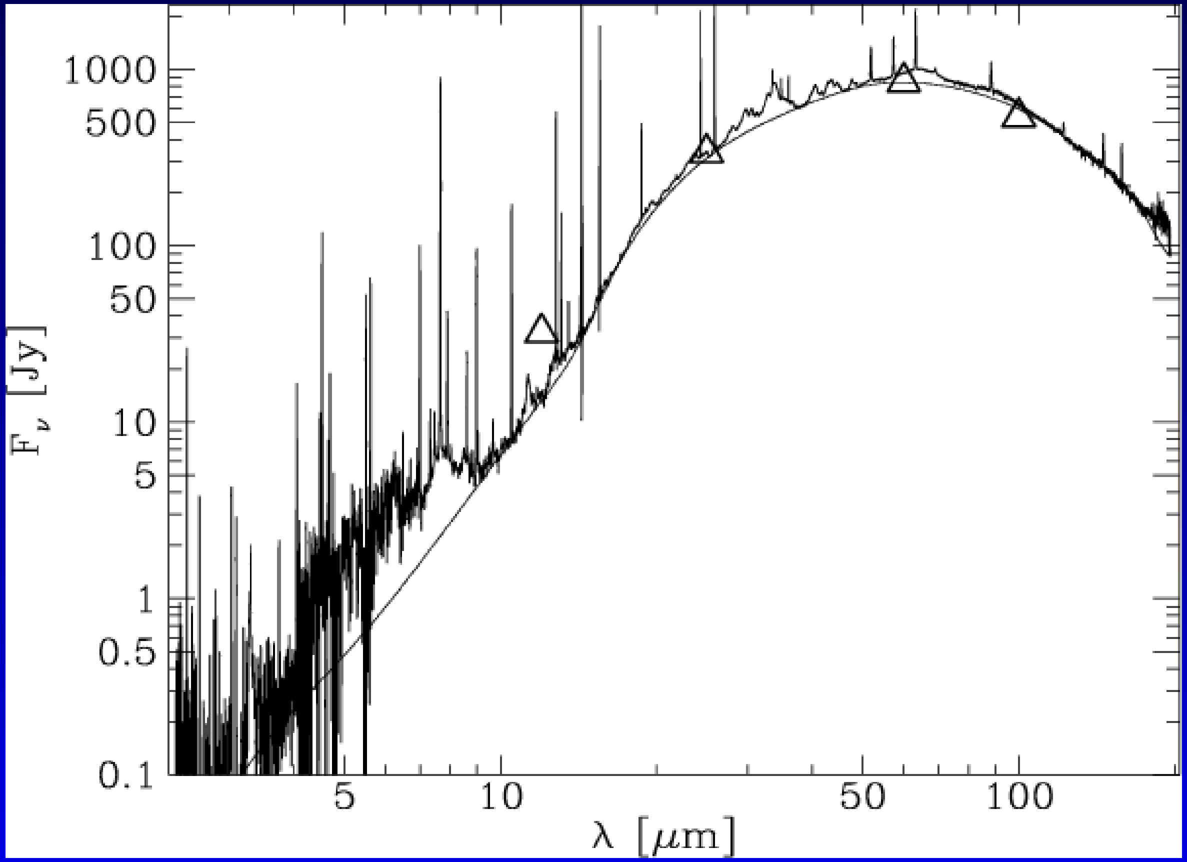

NGC 6302; Molster et al., SWS + LWS spectrum

Dust and Ices

mineral	chemical formula	'60+' band positions [μm]
fosterite	Mg_2SiO_4	69–70
fayalite	Fe_2SiO_4	93–94, 110
diopside	$CaMgSi_2O_6$	65-66
calcite	$CaCO_3$	92
dolomite	$CaMg(CO_3)_2$	62
water ice	H_2O	62
methanol ice	α-CH_3OH	68, 88.5
dry ice	CO_2	85
PAHs "flopping modes"		(far-IR)

Partners involved

Partner	"origin"	hours	special interest
Belgium	PACS GT	145	KUL (AGB, post-AGB, PN, WR, LBV)
			ROB (AGB, PN)
			ULB (binary AGB)
			IAGL (WR, LBV)
Vienna	PACS GT	47	AGB
Heidelberg	PACS GT	10	SN remnants
SAG 6	SPIRE GT	80	SN, AGB, post-AGB, PN
HSC	HSC	26	special type of post-AGB
MS	MS	5	Molecules in specific stars
		—-	
		313	

Implementation (Photo)

PACS:
"Scan Maps" at 70 + 160 μm

78 AGB/RSG, 16 post-AGB/PN, 8 WR/LBV, 5 SN

SPIRE:
"Large maps" at 250, 350, 500 μm

26 AGB/RSG, 8 post-AGB/PN, 5 SN

Implementation (Spectro)

PACS:
Concatenation of two AORs to cover entire 60-210 μm region

Spatial information: 5×5 pixels = $47'' \times 47''$

27 AGB/RSG, 26 post-AGB/PN, 2 WR/LBV, 4 SN

SPIRE:
Complete FTS scan in a single AOR

9 AGB/RSG, 10 post-AGB/PN, 2 WR/LBV, 5 SN

Results

8 papers in the A&A Volume 518 Special Issue (2010)

+ 1 *Nature* paper (2010)

+ Overview paper
(Groenewegen et al. 2011, A&A 526, A162)

+ 8 other refereed papers

-Massive stars

-SNe

-PNe

In more detail:

-AGB imaging

-AGB spectroscopy

Massive stars

TARGET	PACS	PACS	SPIRE	SPIRE	PARALLEL	
	PHOT	SPEC	PHOT	SPEC		
AG CAR	2202927-30	RC 2197792-93		2189114	2203081-82	A
					2211615-16	
					2255061-62	
WRAY 15-751	2188849-52	RC 2187236-37			2203081-82	B
HEN 3-519	2188511-13				See AG CAR	A
	2202931-34					
HR CAR	2203101-04	LU 2247817-18			2255011, 5060	E
HD 168625	2217763-66	RC 2229740-41			2218997-98	E
GAL 79.29+0.46	2196767-70	LU 2235692-93			2196917-18	E
	2187795-98		2187718		2211307-08	
					2244168-69	
PN M1-67	2194080-83	LC 2220598-99	2204949	2192828		A
NGC 6888	2194049-50	LU 2256927-28*				C
	2212040-43	LU 2256477-78*				
NGC 6164/5	2227809-12	LU 2252090-93			2204056-57	D

R/L : Range/Line C/U : Chopped/Unchopped *OT2_dstock_3

Chloi Vamvatira-Nakou (Ph.D.)
D. Hutsemekers, P. Royer

MESSive STARS – Wray15-751

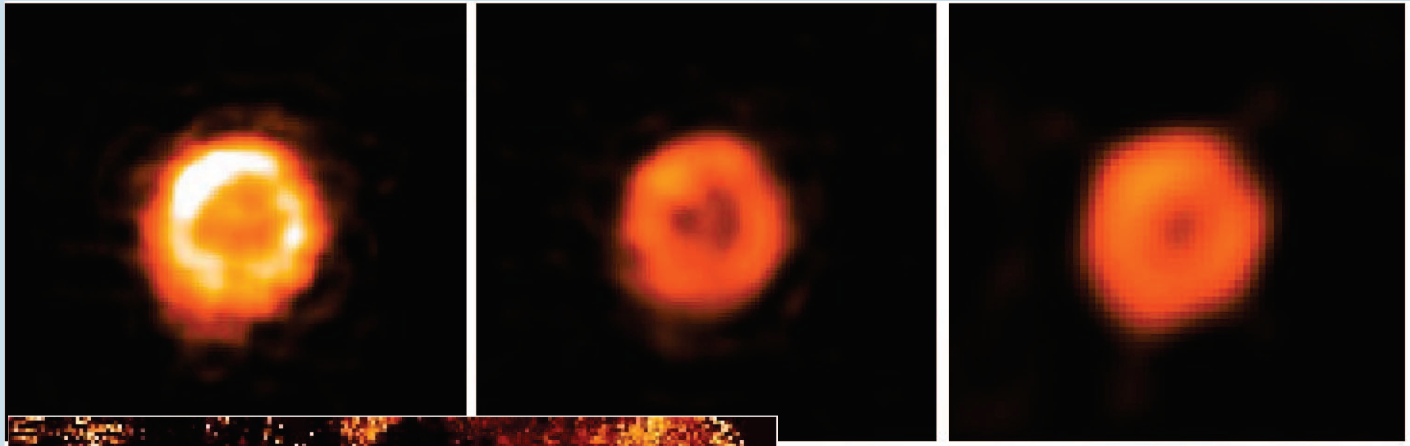

MSC deconvolutio
(Magain et al.)

Inner ring radius ~

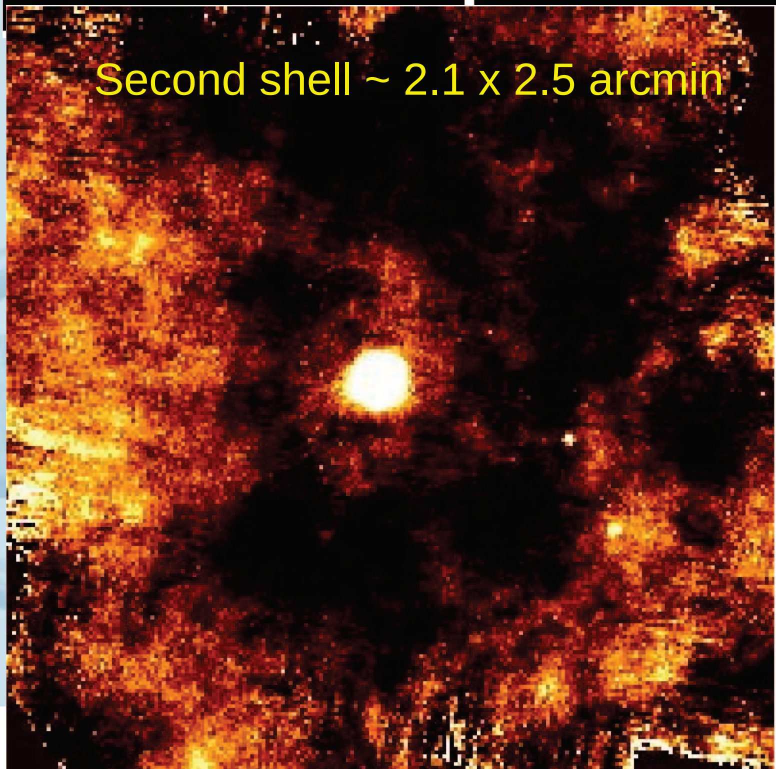

Dust Nebula modeled with 2-Dust

- → compare IRAS/ISO to Akari/Herschel
- → no significant change in Dust emission 1996 – 2010
- → Stellar variations occur at cst L

Spectroscopic Analysis

- → Abundances
- → PDR characteristics
- → Dust & gas mass estimates
- → M-Loss history

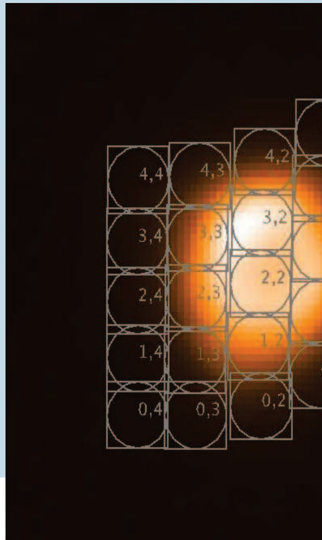

The Herschel MESS Supernova Programme

Targets: 4 historical supernova remnants in the Mill Way

			$M_{(dust)}$ (T_d<50K)	
1680	IIb	Cas A	**0.10 Msun**	**Barlow et al (2010)**
1604	Ia	Kepler	**0.003 Msun**	**Gomez et al (2012a**
1572	Ia	Tycho	**0.009 Msun**	**Gomez et al (2012a**
1054	II	Crab	**0.10-0.24 Msun**	**Gomez et al (2012b**

All young: so swept-up interstellar gas mass is low

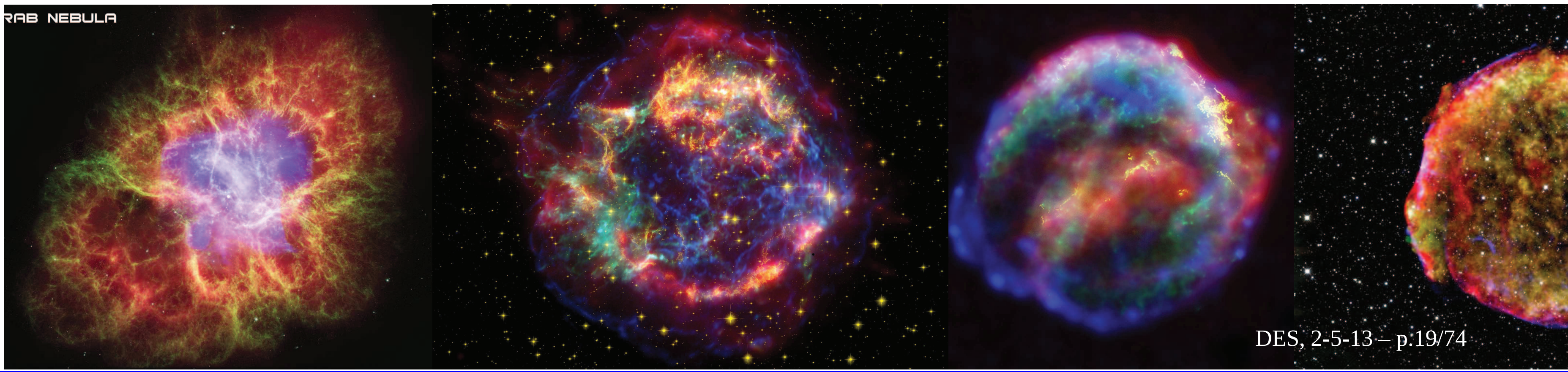

SN remnant: Cas A

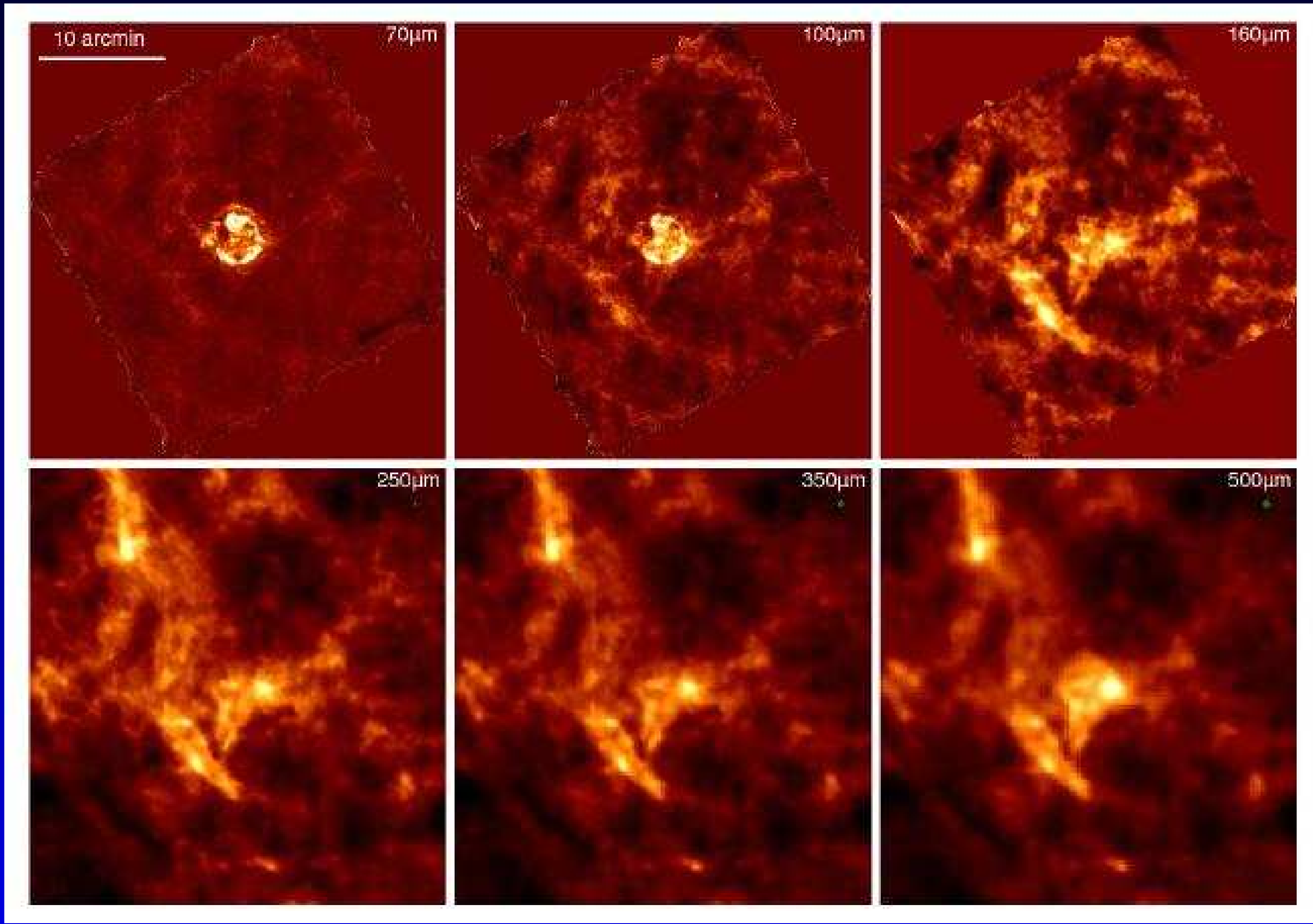

Barlow et al. (2010)

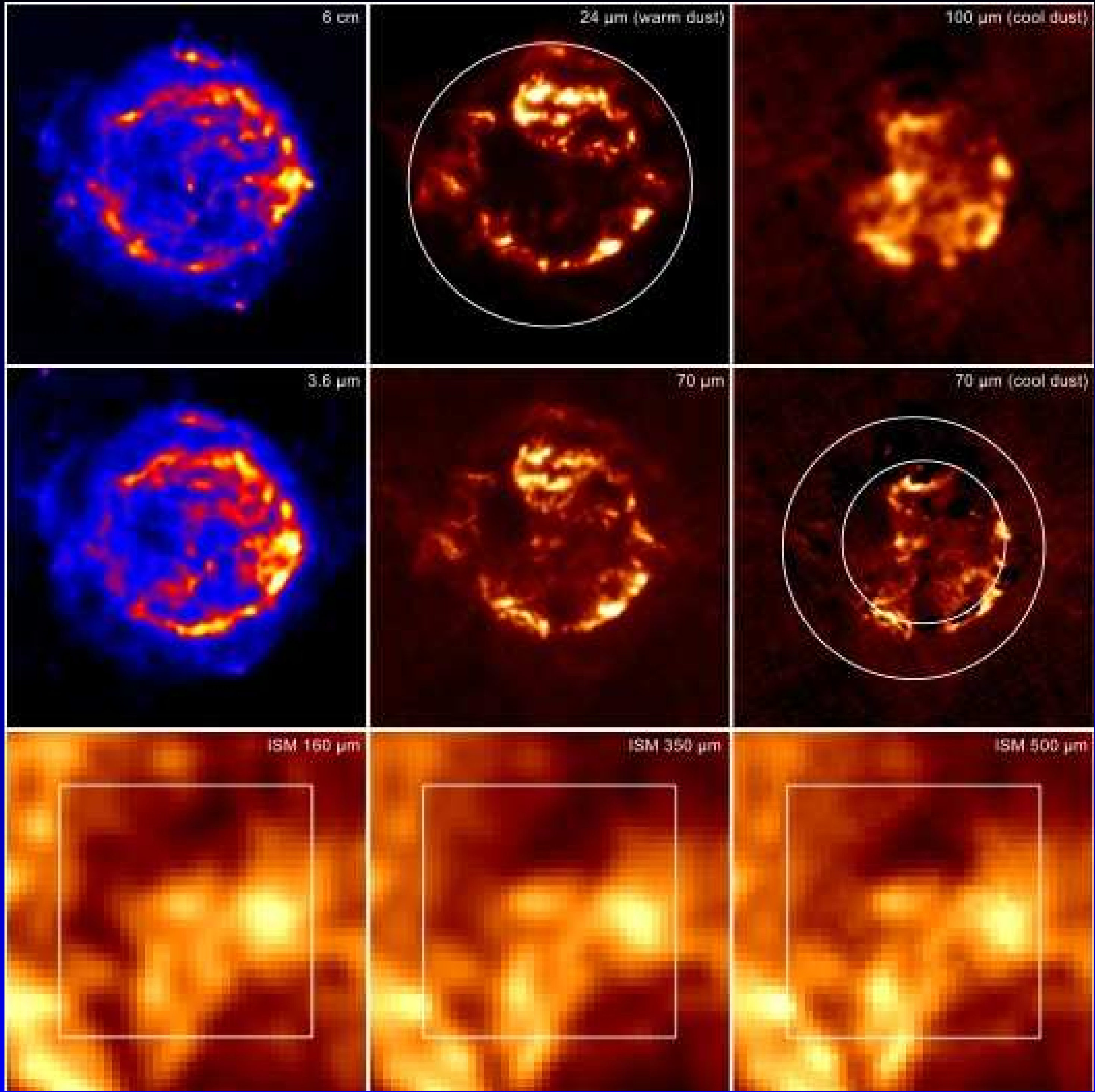
6 cm
24 µm (warm dust)
100 µm (cool dust)
3.6 µm
70 µm
70 µm (cool dust)
ISM 160 µm
ISM 350 µm
ISM 500 µm

SN remnants

- non-thermal component: based on 6-cm VLA and 3.6-μm IRAC image (*Planck*, *WISE*)
- line contributions: dedicated PACS/SPIRE spectroscopy & archival LWS spectrum (Cas A: $\sim 5\%, \sim 10\%$ neglegible at 70,100,160 μm)

Crab A: T= 56 K, M= 0.008 $M_{\odot}$; T= 28 K, M= 0.24 $M_{\odot}$ (silicates)

Cas A: T= 82 K, M= 0.003 $M_{\odot}$; T= 35 K, M= 0.08 $M_{\odot}$

Kepler: T= 82 K, M= 0.003 $M_{\odot}$; cool comp, M $<$0.07 $M_{\odot}$

Tycho: T= 90 K, M= 0.009 $M_{\odot}$; cool comp, M $<$0.07 $M_{\odot}$

"...that significantly less dust forms in the ejecta of Type Ia supernovae than in the remnants of core-collapse explosions."

Planetary Nebulae

Imaging:
NGC 650, 3587, 6543, 6720, 6853, 7027, 7293

Spectroscopy:
NGC 6302, 6537, 6543, 7027

NGC 6720 (van Hoof et al. 2010);
NGC 650, NGC 7027 (advanced drafts)

Time consuming:
-Cloudy modelling
-Adding loads of literature data (different apertures...)

NGC 6720

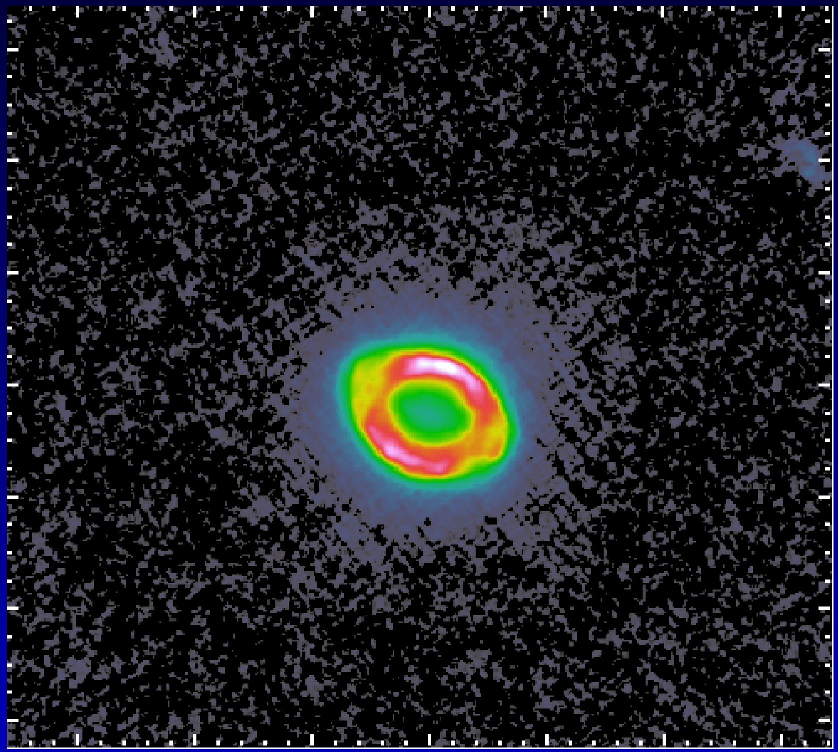

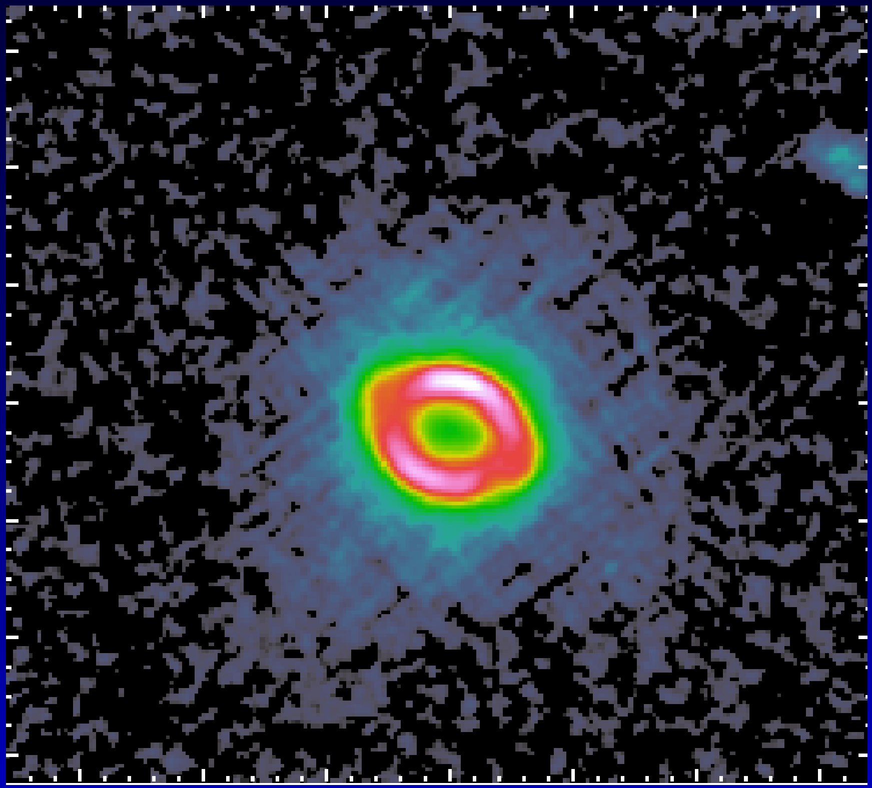

van Hoof et al. (2010)
PACS 60 and 160 micron

NGC 6720: H_2 formation on dust grains

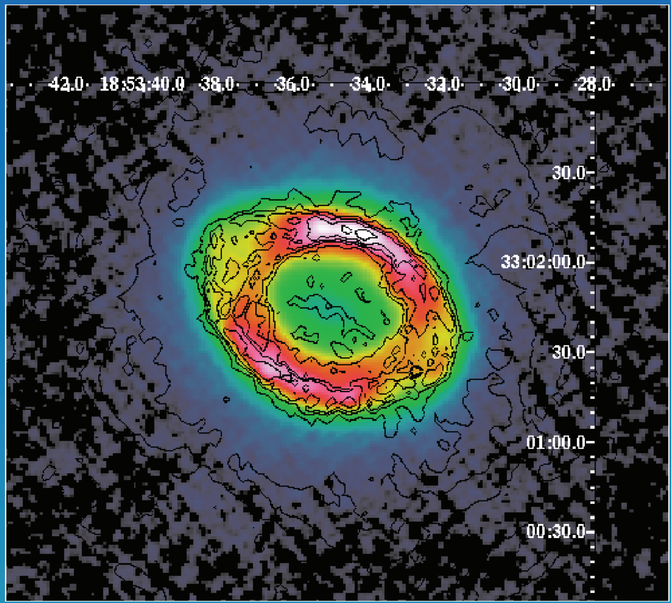

Overlay of the H_2 2.12 µm emission (contours) on the PACS 70 µm image of NGC 6720 showing the dust emission. The detailed match between the H_2 and dust emission appears to be the first observational evidence that H_2 forms on oxygen-rich dust grains.

- We have developed a photoionization model of the nebula with the Cloudy code, which we used to investigate possible formation scenarios for H_2.
- We conclude that the most plausible scenario is that the H_2 resides in high density knots which were formed after the recombination of the gas started when the central star luminosity dropped steeply around 1000-2000 years ago.
- The models show that H_2 formation in the knots is expected to be substantial since then, and may well still be ongoing at this moment.
- van Hoof et al. 2010, A&A, 518, L137

AGB star imaging

- "detached shell" objects
- influence of binarity
- CW Leo
  - bow shock
  - inner parts
  - phase-lag distance
- Betelgeuze and its environment
- interaction CSE with the ISM

Detached shells

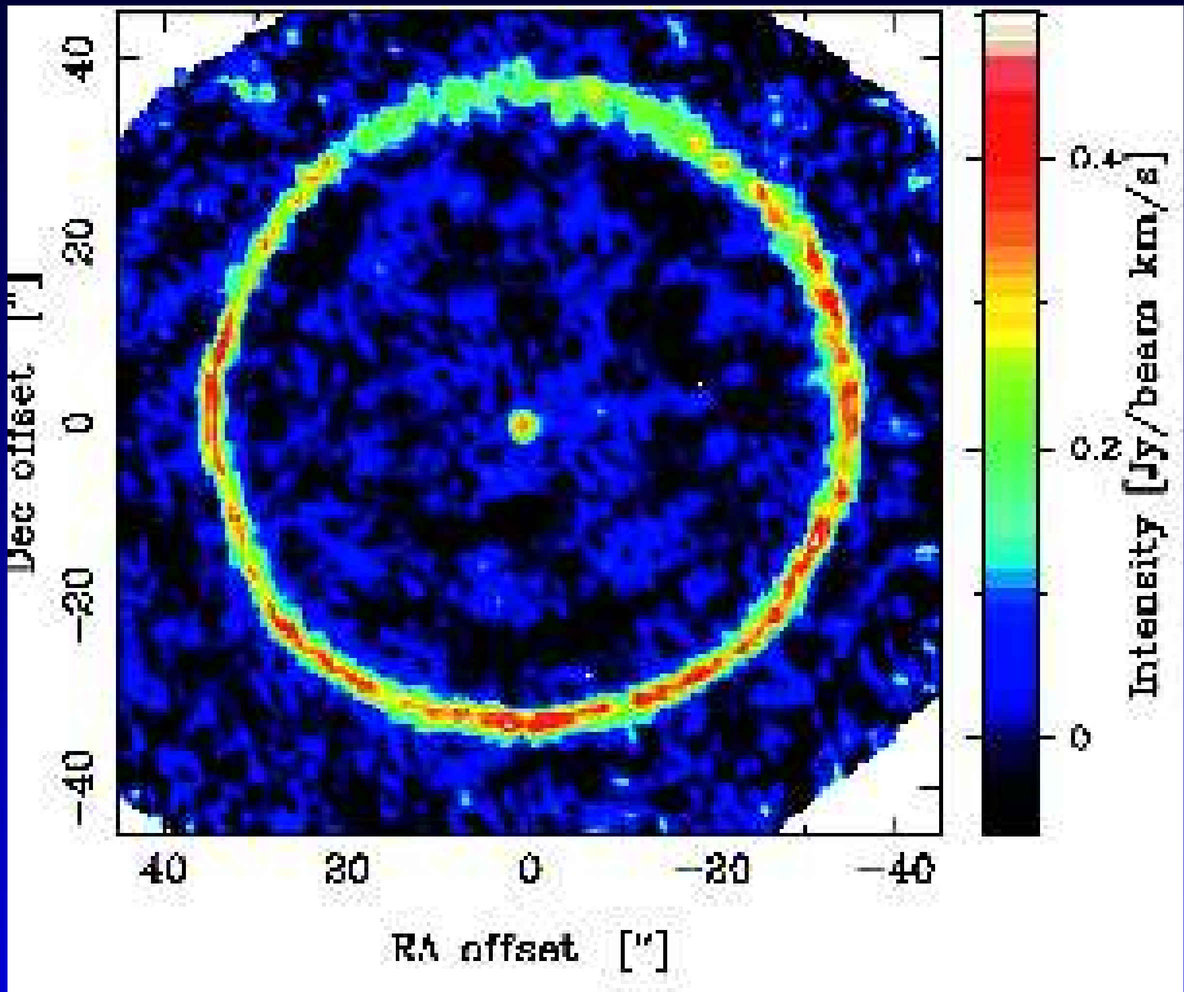

TT Cyg; Olofsson et al. (2000). PdB CO (1-0)
Short-duration large mass-loss rate event

Detached shells

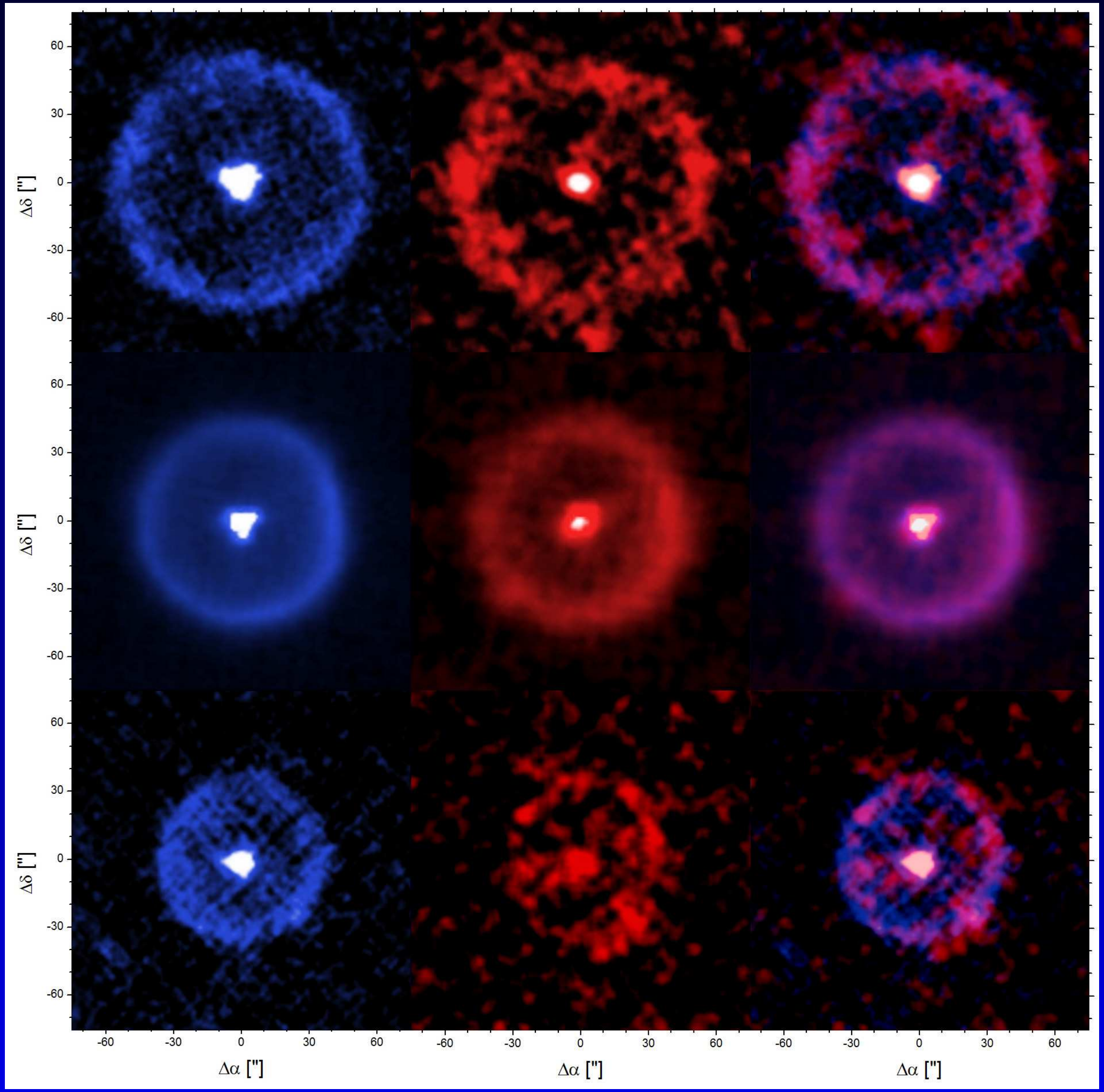

Kerschbaum et al. (2010)

PACS: blue / red / combined

AQ And, U Ant, TT Cyg

Detached shells

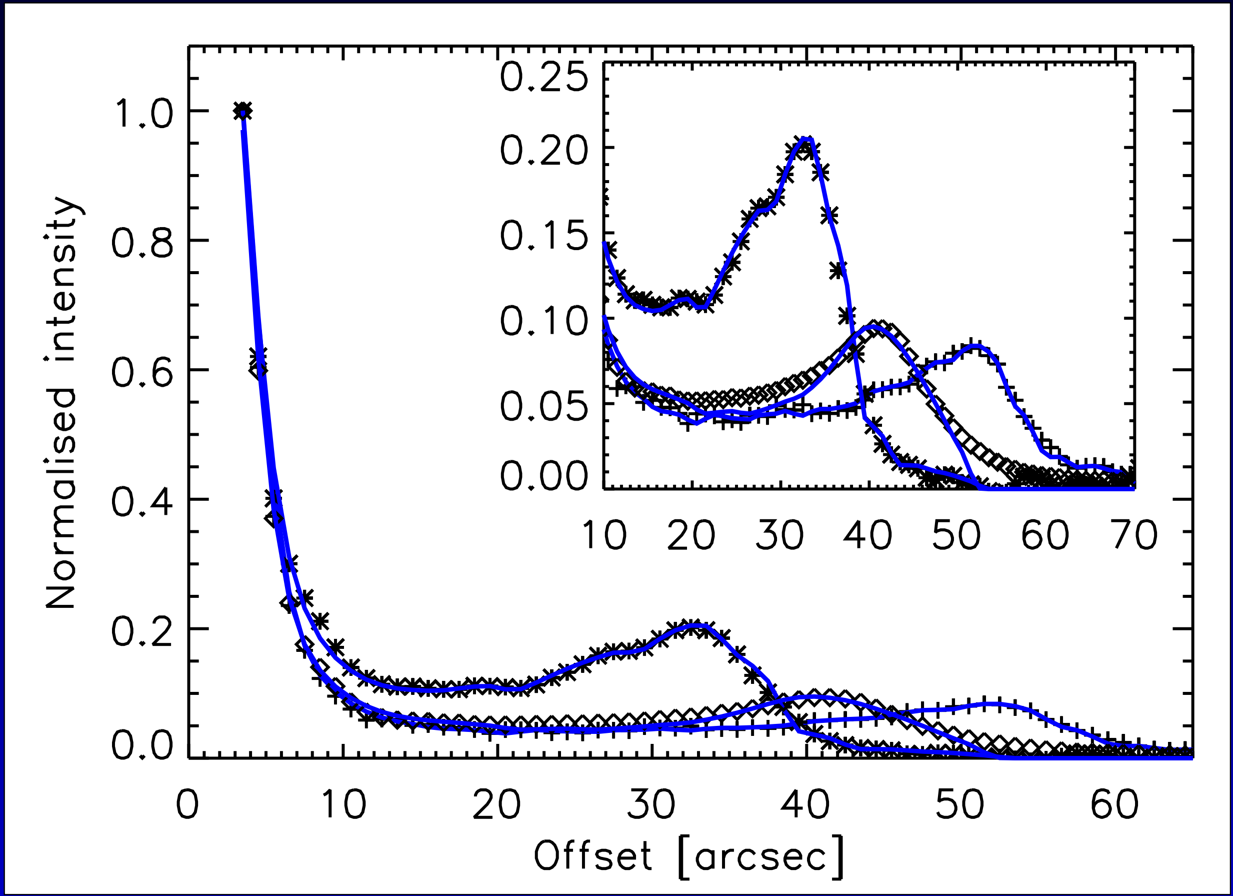

AQ And=+
U Ant=◇
TT Cyg=×

DUSTY multiple-shells $T_{\rm dust}$ = 25-50 K

Kerschbaum et al. (2010, A&A Special Issue)

MoD - More of DUSTY

- Improved DUSTY
  (discontinuous density distribution, $\sim r^{-p}$)
- embedded DUSTY code into a minimisation routine
- Can fit photometry, spectra, intensity distributions and visibility data
- 2012, A&A 543, A36
- AQ And: 7 parameters
  L, $\tau_{\rm V}$, $R_{\rm in,shell}$, $\Delta R_{\rm shell}$, $p_{\rm o}$, $p_{\rm shell}$, "density jump"

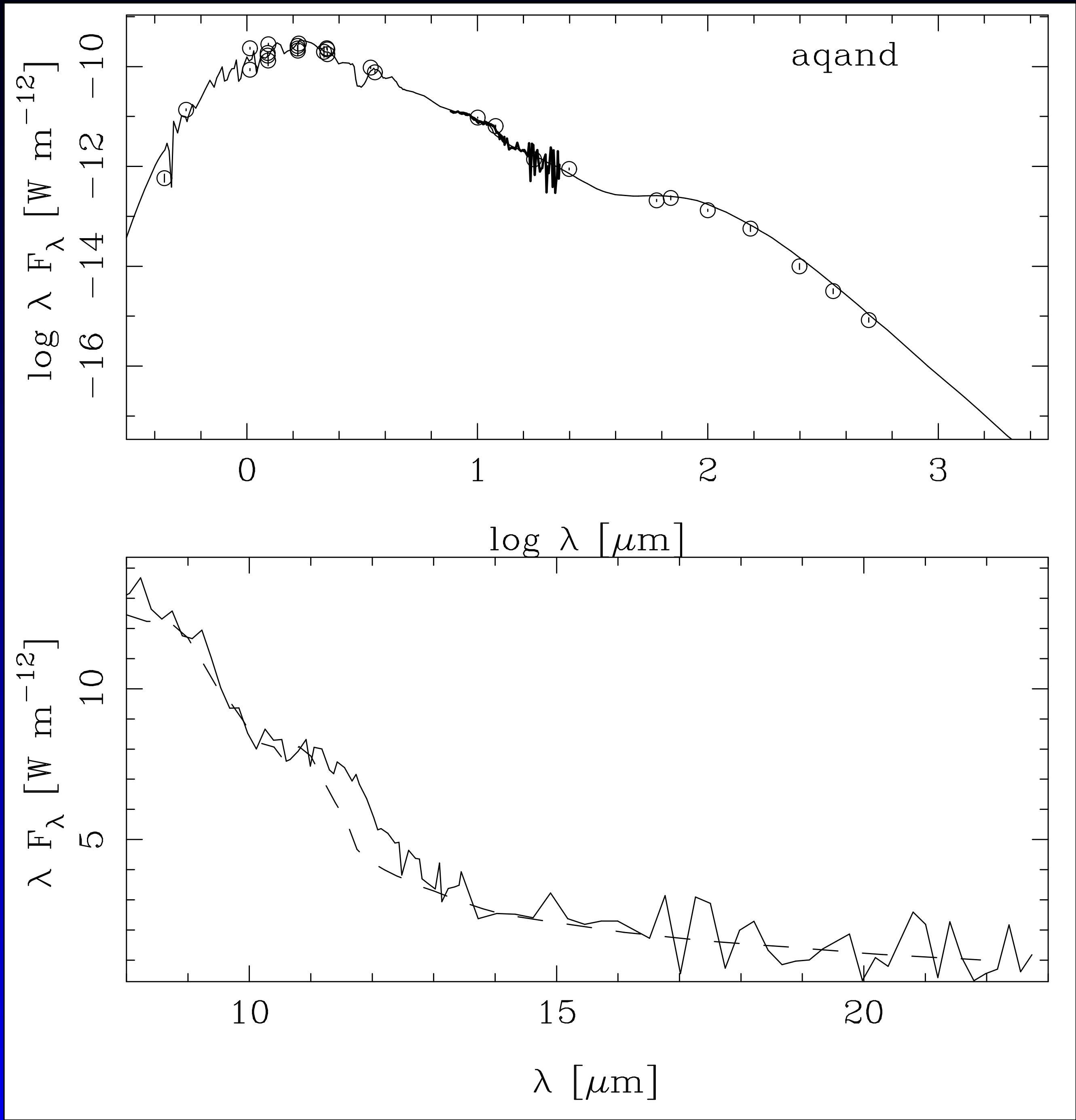
aqand
log λ F$_\lambda$ [W m^{-12}]
−16
−14
−12
−10
0
1
2
3
log λ [μm]
λ F$_\lambda$ [W m^{-12}]
5
10
10
15
20
λ [μm]

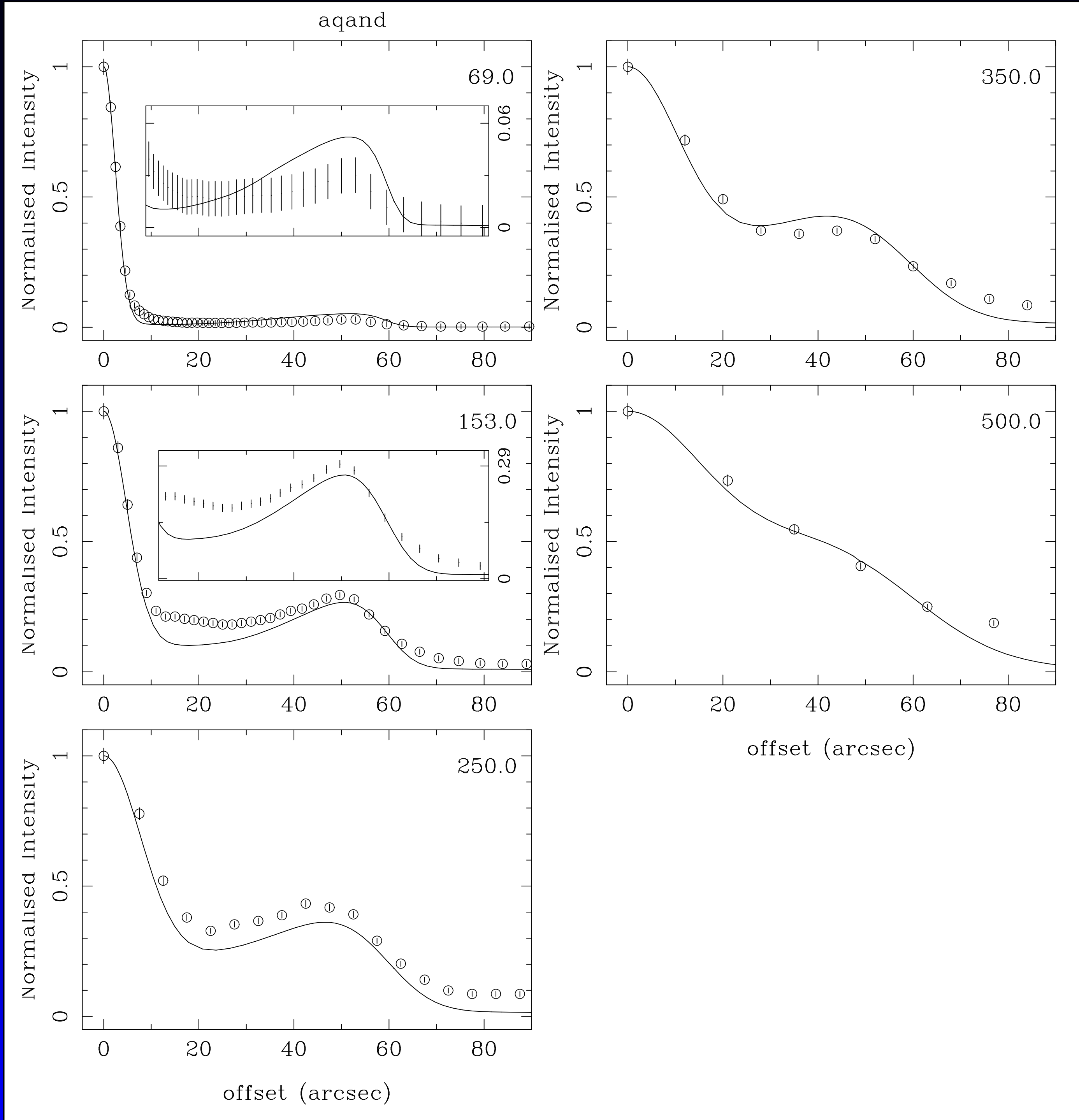
aqand
69.0
350.0
153.0
500.0
250.0
Normalised Intensity
offset (arcsec)
0
0.5
1
0.06
0.29
20
40
60
80

ALMA - Synergy

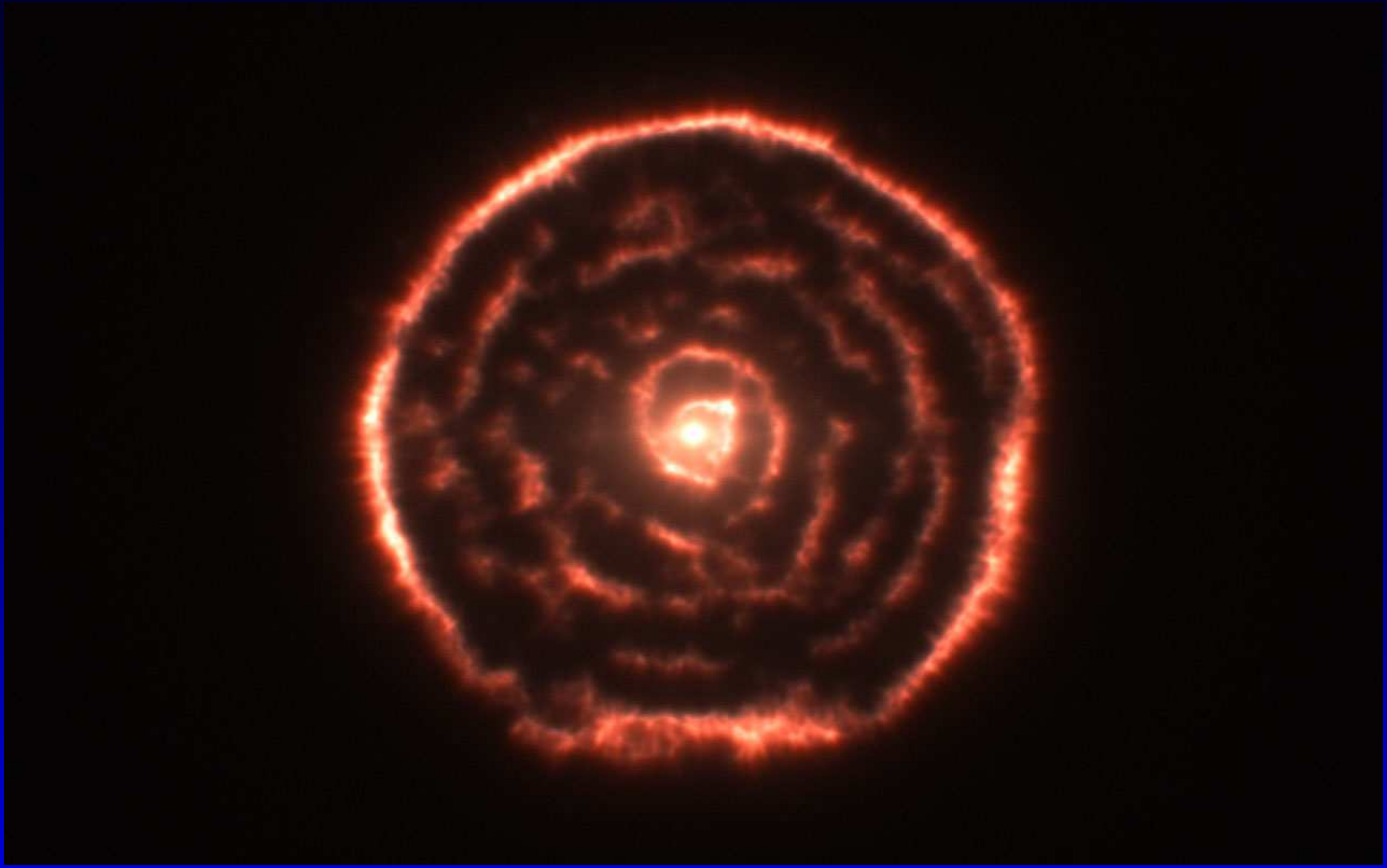

Maercker et al. (2012, Nature 490, 232)
R Scl CO(3-2) 40″x 40″

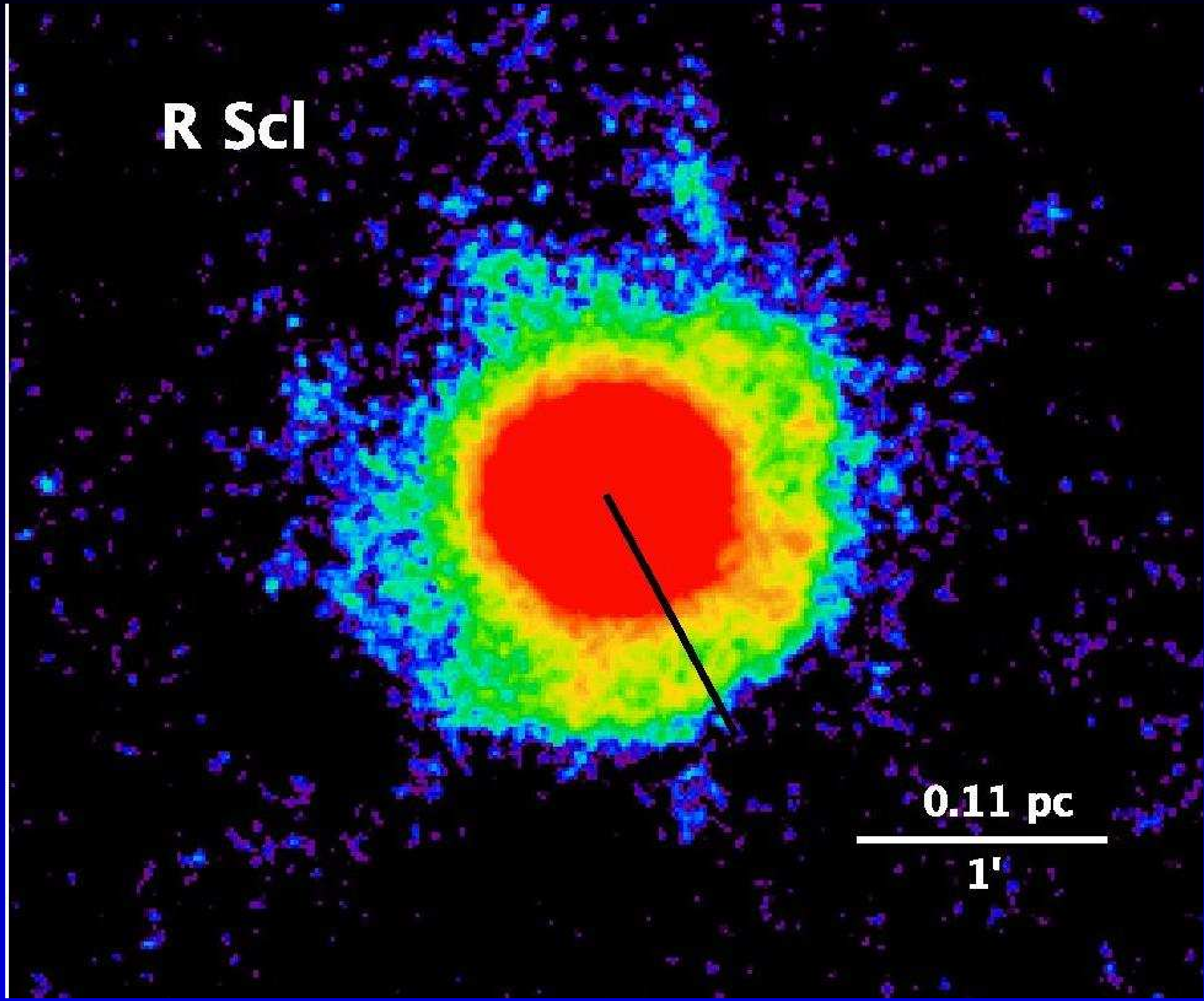

Herschel view at 70 μm. Note different spatial scale !!

Binarity

"Herschel’s view into Mira’s head",
Mayer, Jorissen et al. (2011)

R Aql & W Aqr; Mayer, Jorissen et al. (2013)

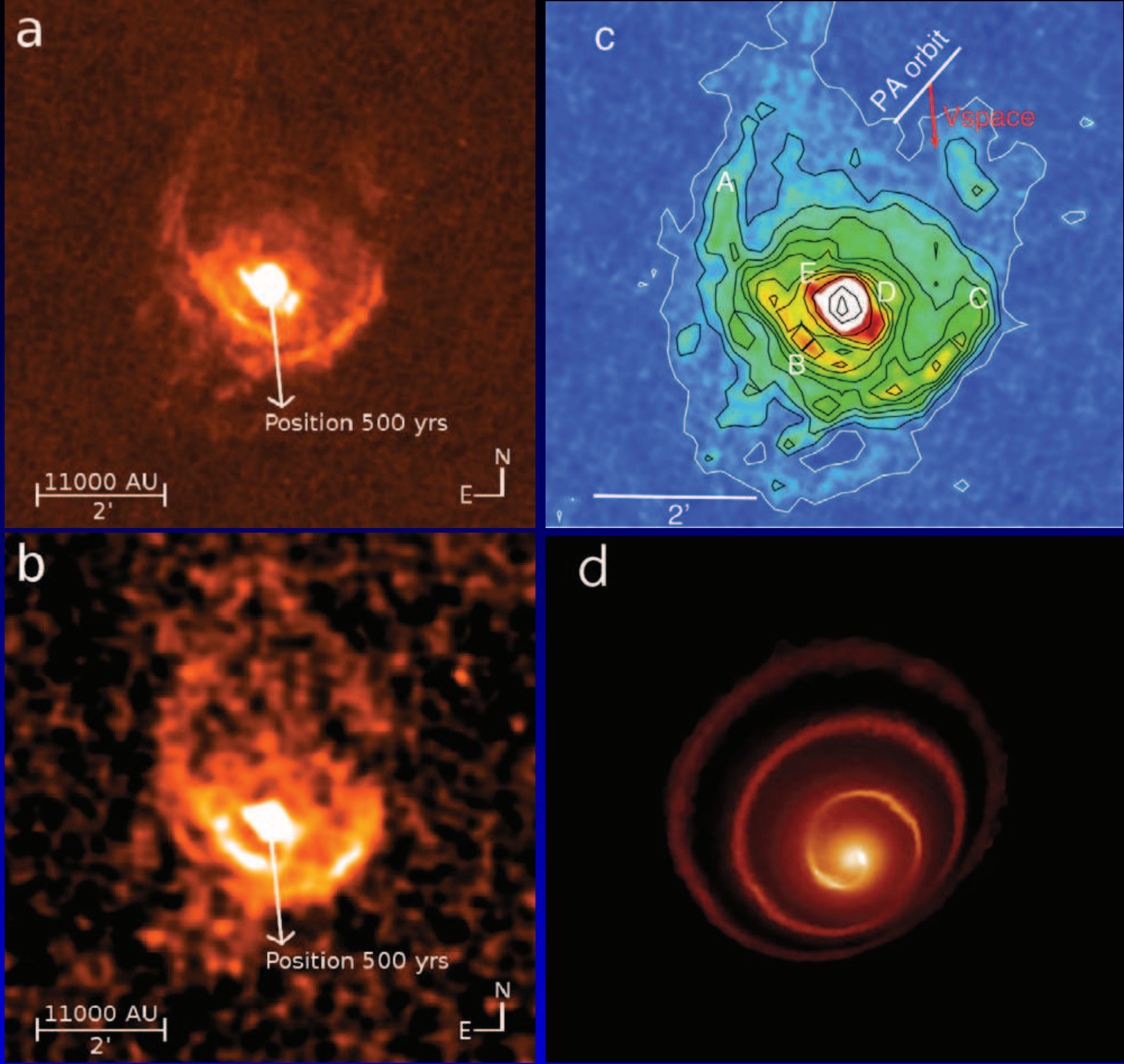

Mira (a) deconvolved 70 μm image, (b) deconvolved 160 μm image, (c) deconvolved 70 μm image with countours and arcs labelled, (d) toy model

Mira

"The overall shape of the IR emission around Mira deviates significantly from the expected alignment with Mira’s exceptionally high space velocity.

...

By comparing Herschel and GALEX data, we found evidence for the disruption of the IR arcs by the fast outflow visible in both Hα and the far UV.

...

Mira’s IR environment appears to be shaped by the complex interaction of Mira’s wind with its companion, the bipolar jet, and the ISM. "

CW Leo - bowshock

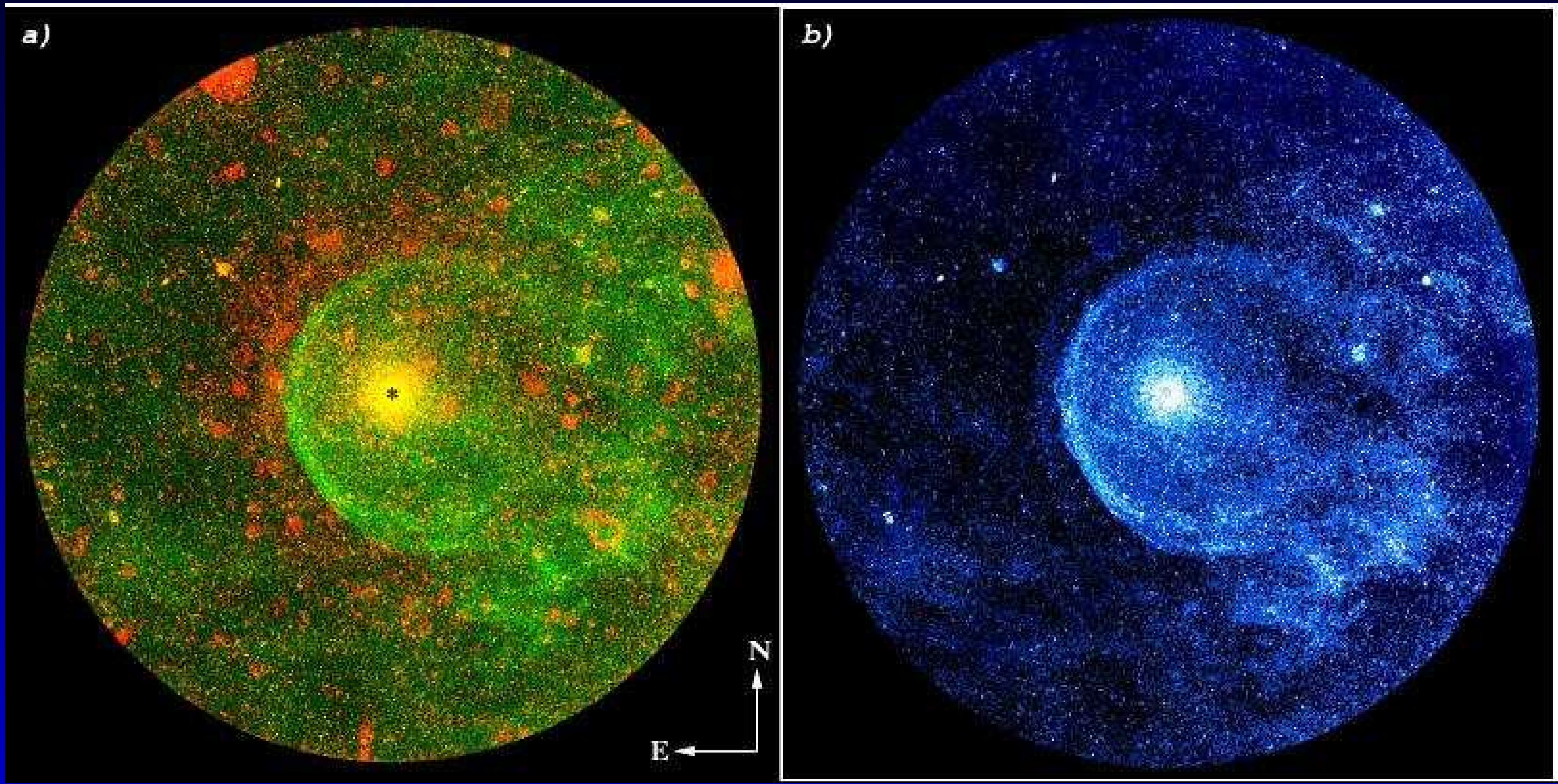

GALEX NUV/FUV composite (left), FUV (right).
Sahai & Chronopoulos (2010)

CW Leo - bowshock

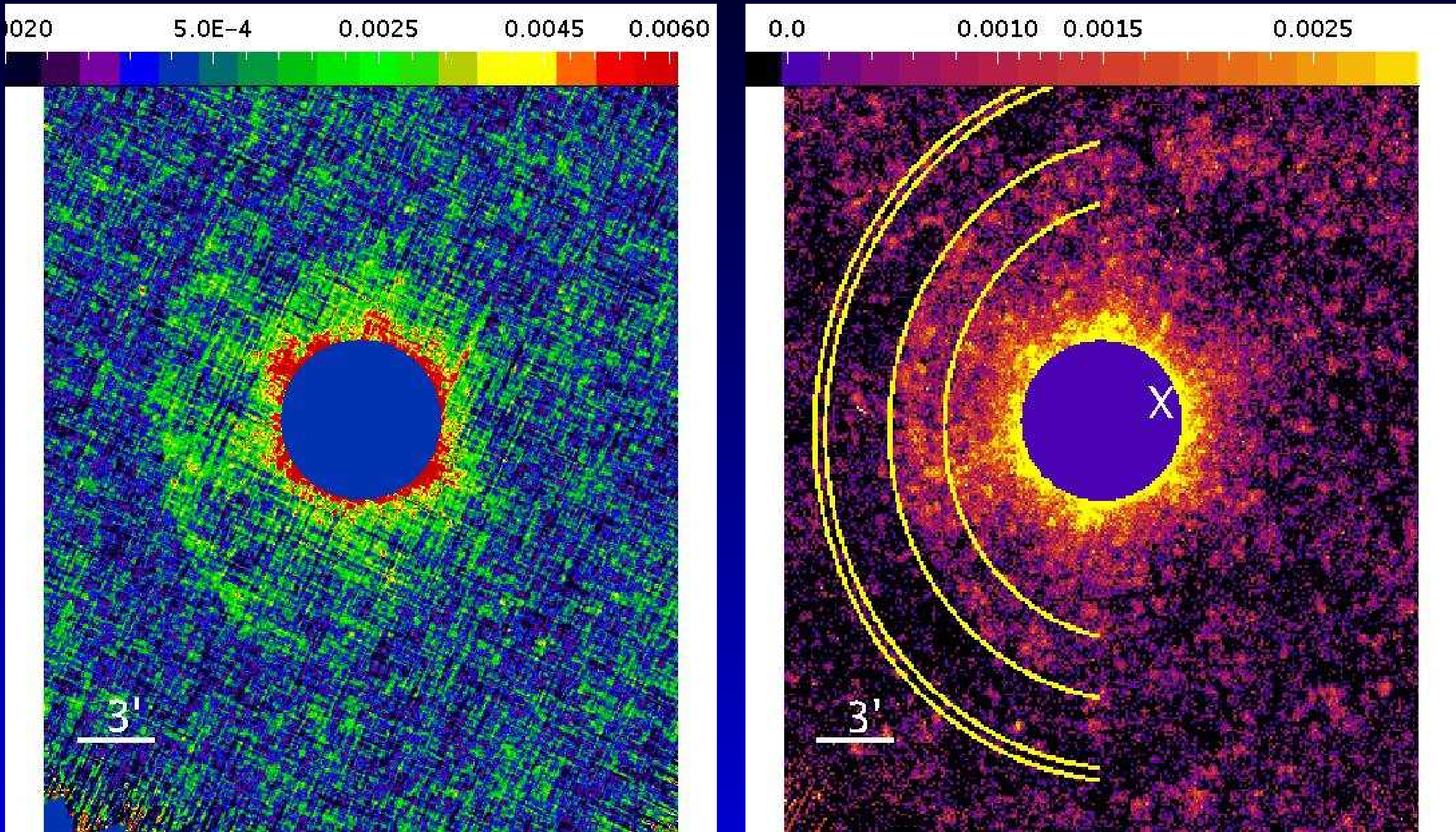

PACS 160 and SPIRE 250 micron
$23' \times 27'$ (Ladjal et al. 2010)

CW Leo - bowshock

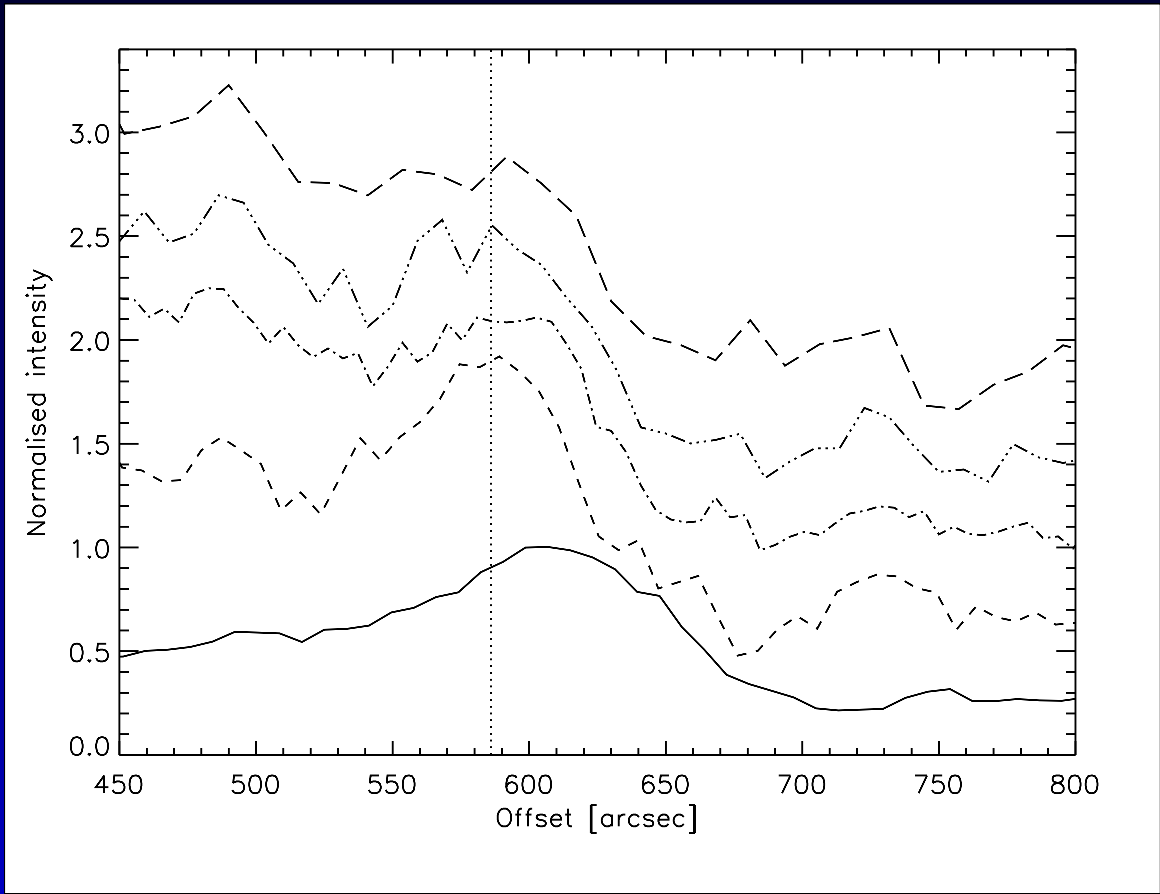

Intensity profiles FUV, 160, 250,350,550 micron

$T_{\mathrm{dust}} = 25$ K $\quad V_{\star\mathrm{relativeISM}} = 107/\sqrt{n_{\mathrm{ISM}}}$ km s^{-1}

CW Leo - inner part

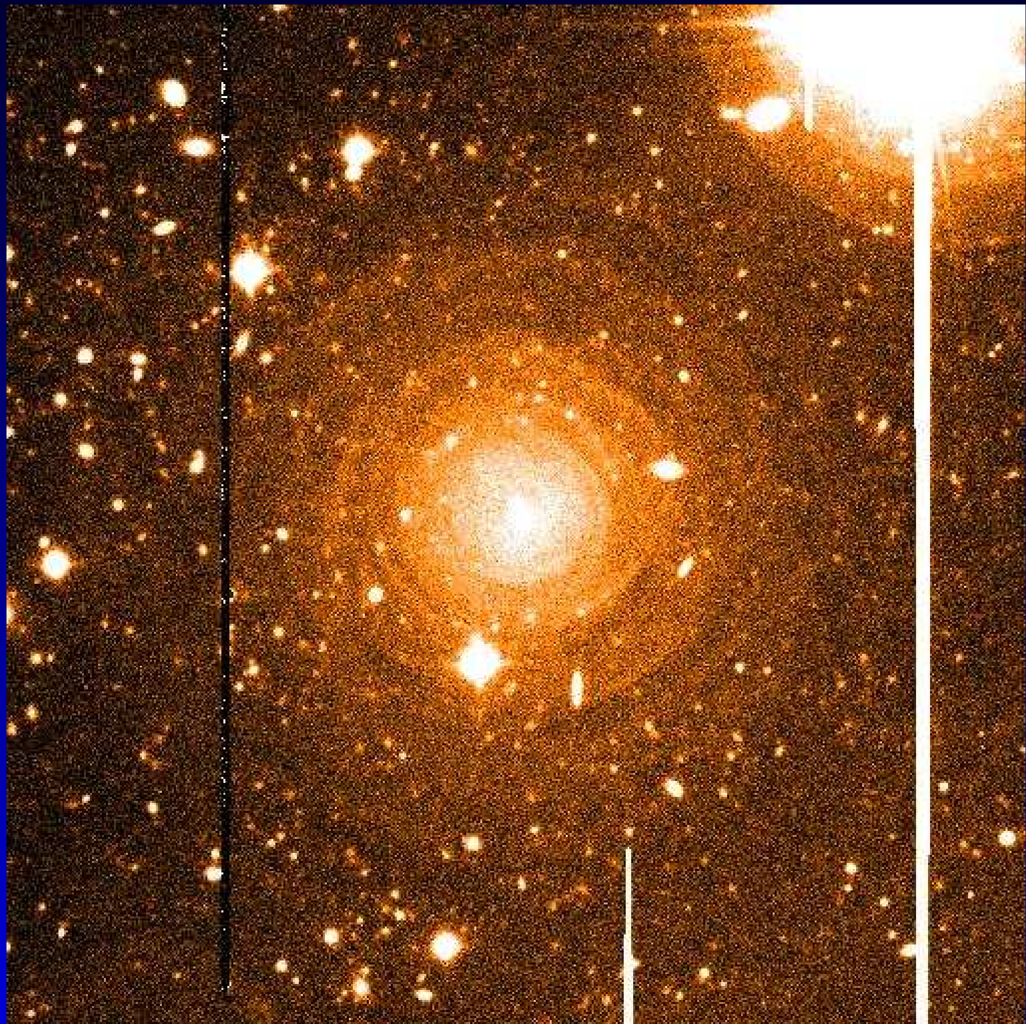

(Mauron & Huggins 1999) *V*-band, FoV= 223 x 223″

CW Leo - inner part

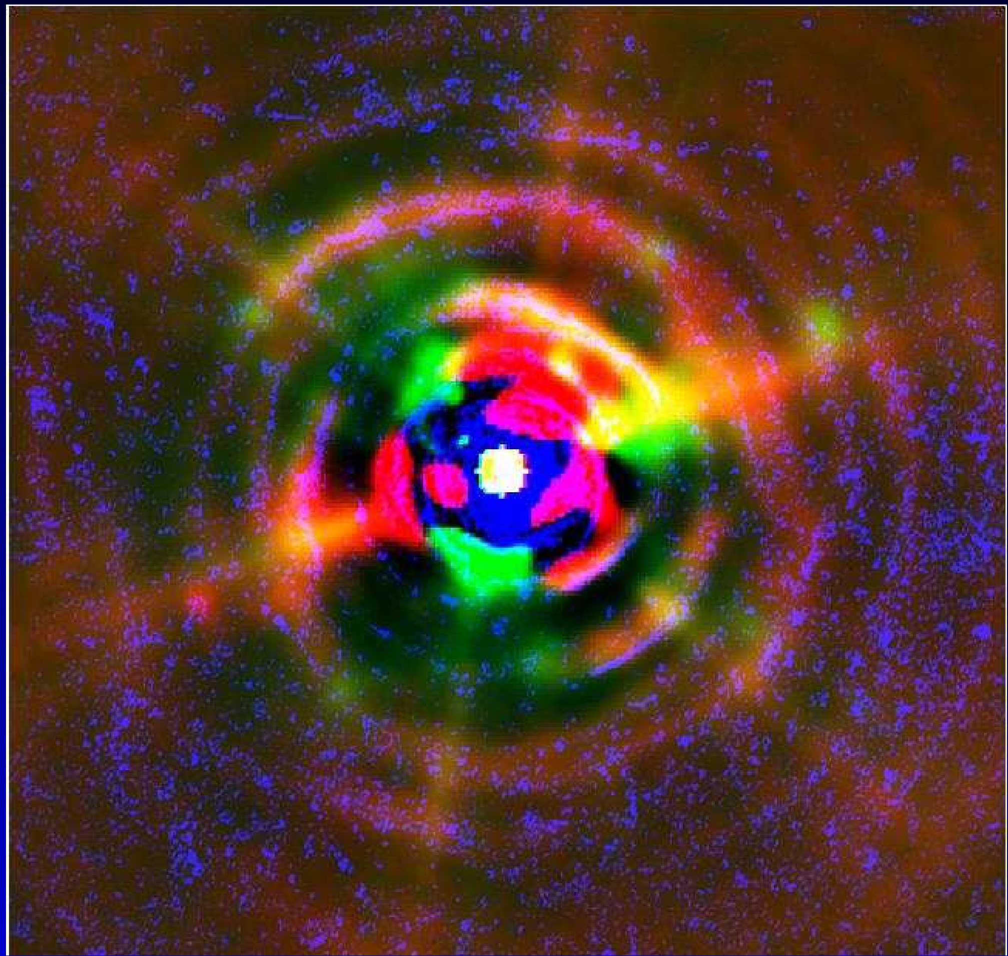

Combined image of the PACS 70 μm (green), PACS 100 μm (red) and V-band (blue).
FoV= 204 x 204$''$

Decin et al. (2011)
non-isotropic mass-loss events and clumpy dust formation

CW Leo - inner part

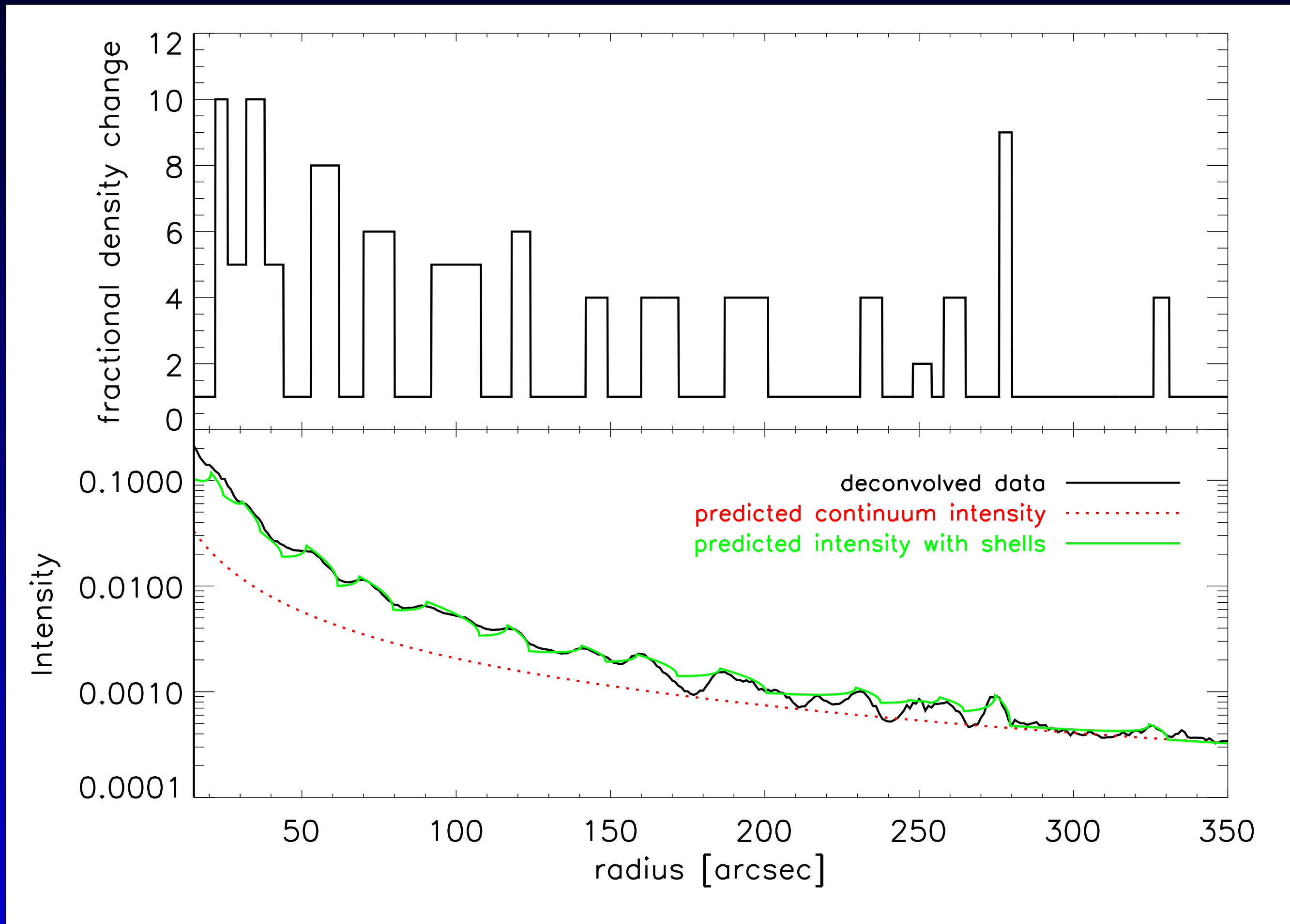

A model (Decin et al. 2011)

CW Leo - inner part

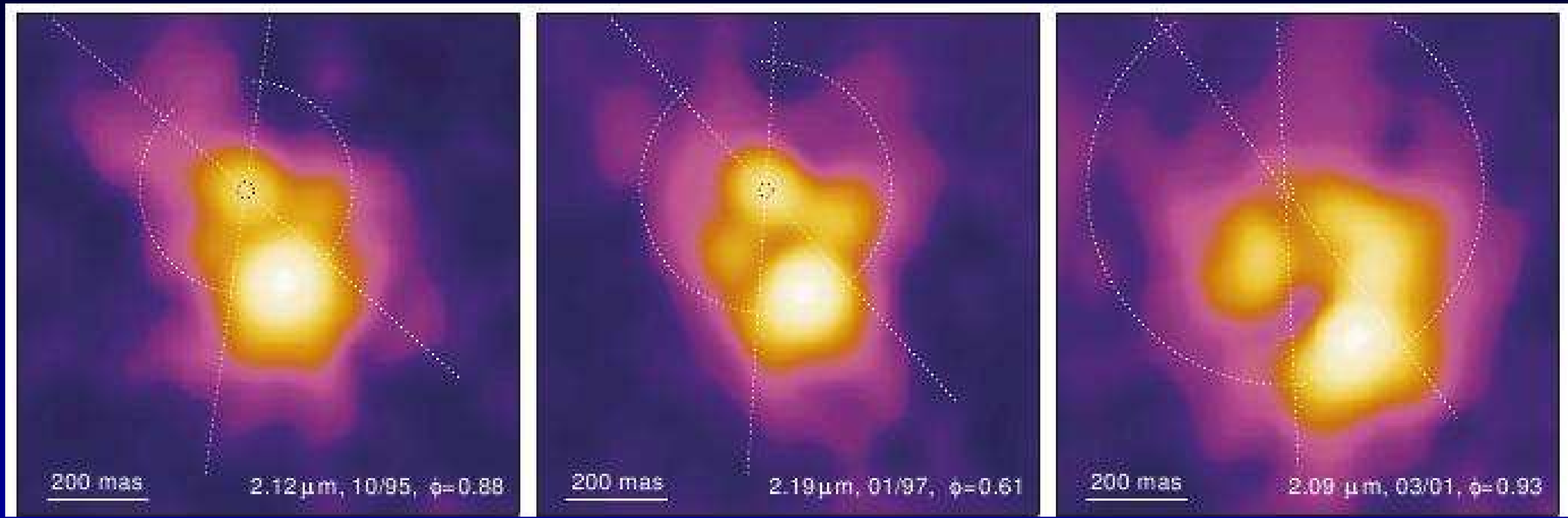

(Menshchikov et al. 2002) K-band speckle
FoV= 1 x 1″

CW Leo - Distance

CW Leo (= IRC +10 216 = AFGL 1381)
Two-micron Sky Survey (Becklin et al. 1969)

d = 110-135 pc (Groenewegen et al. 1998)
Dust and molecular radiative-transfer models were used to fit simultaneously the available photometric data, the *IRAS* LRS spectrum, near- and mid-IR interferometric observations, and CO J= 1-0 up to 6-5 molecular line emission data.

Pulsation Period: 644 $\pm$ 17 days (Witteborn et al. 1980), 636 $\pm$ 3 days (Ridgway & Keady 1988), 638 days (Dyck et al. 1991)

5 epochs (2 MESS + 3 DDT (PI. Groenewegen))

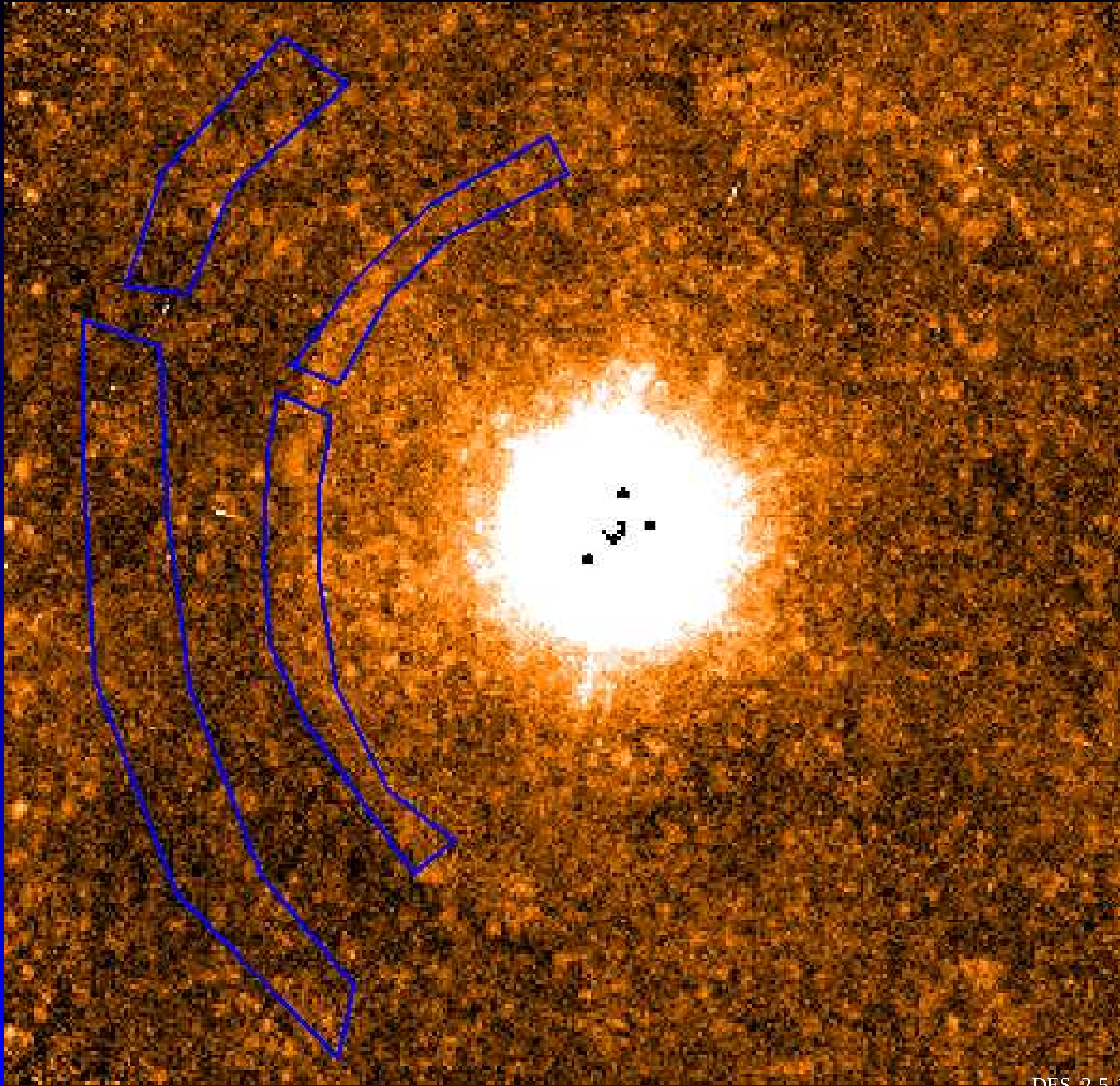

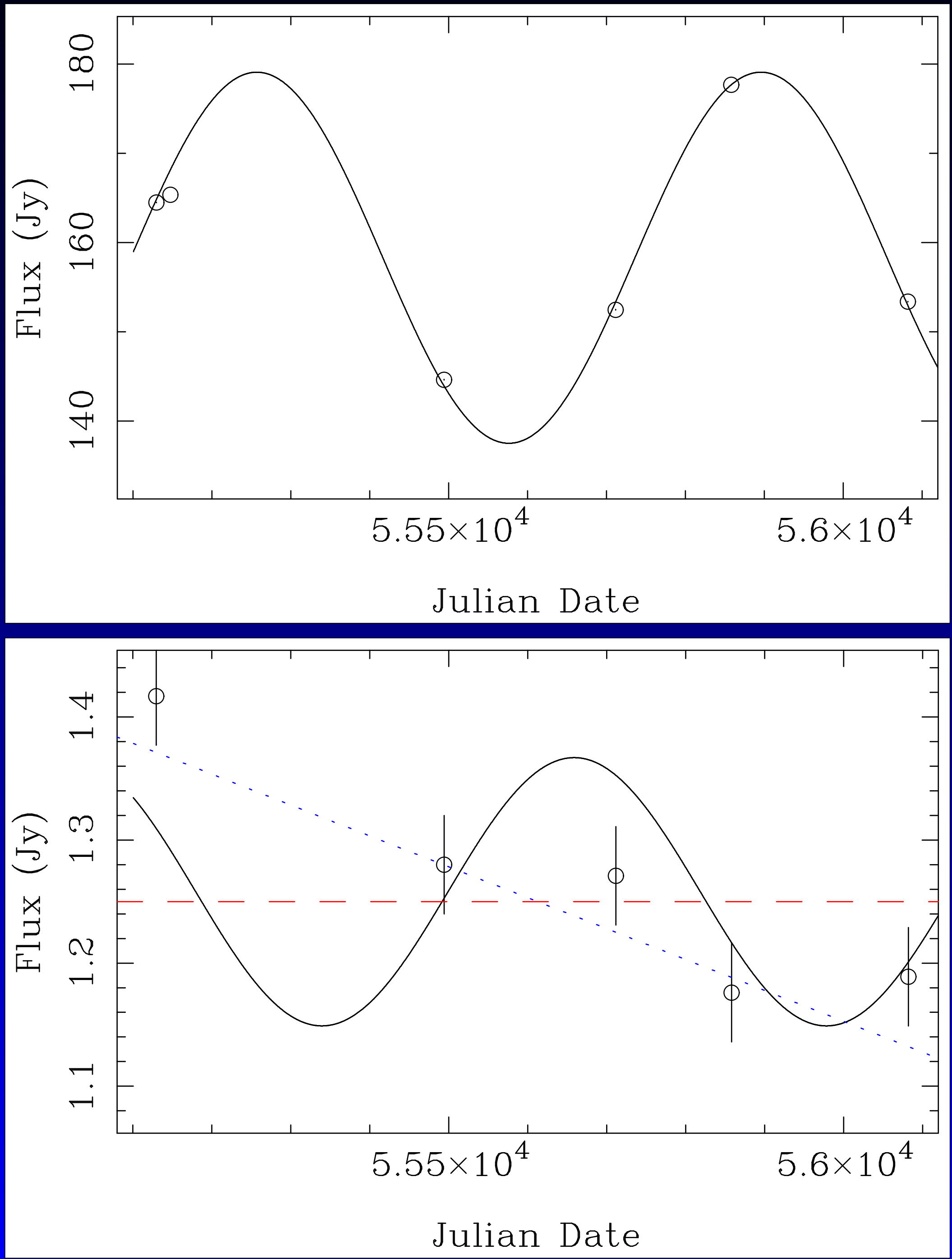

Groenewegen et al. (2011)

The phase lag of (402 ± 37) days

CW Leo - Distance

Angular separation between the emission of the central star and the bow shock is $(534 \pm 16)''$.

If the bow shock were located in the plane-of-the-sky, the distance to CW Leo would follow immediately as d = 130 $\pm$ 13 pc. And this is a strict upperlimit.

Can one do better?

INTERMEZZO !

Interaction ISM

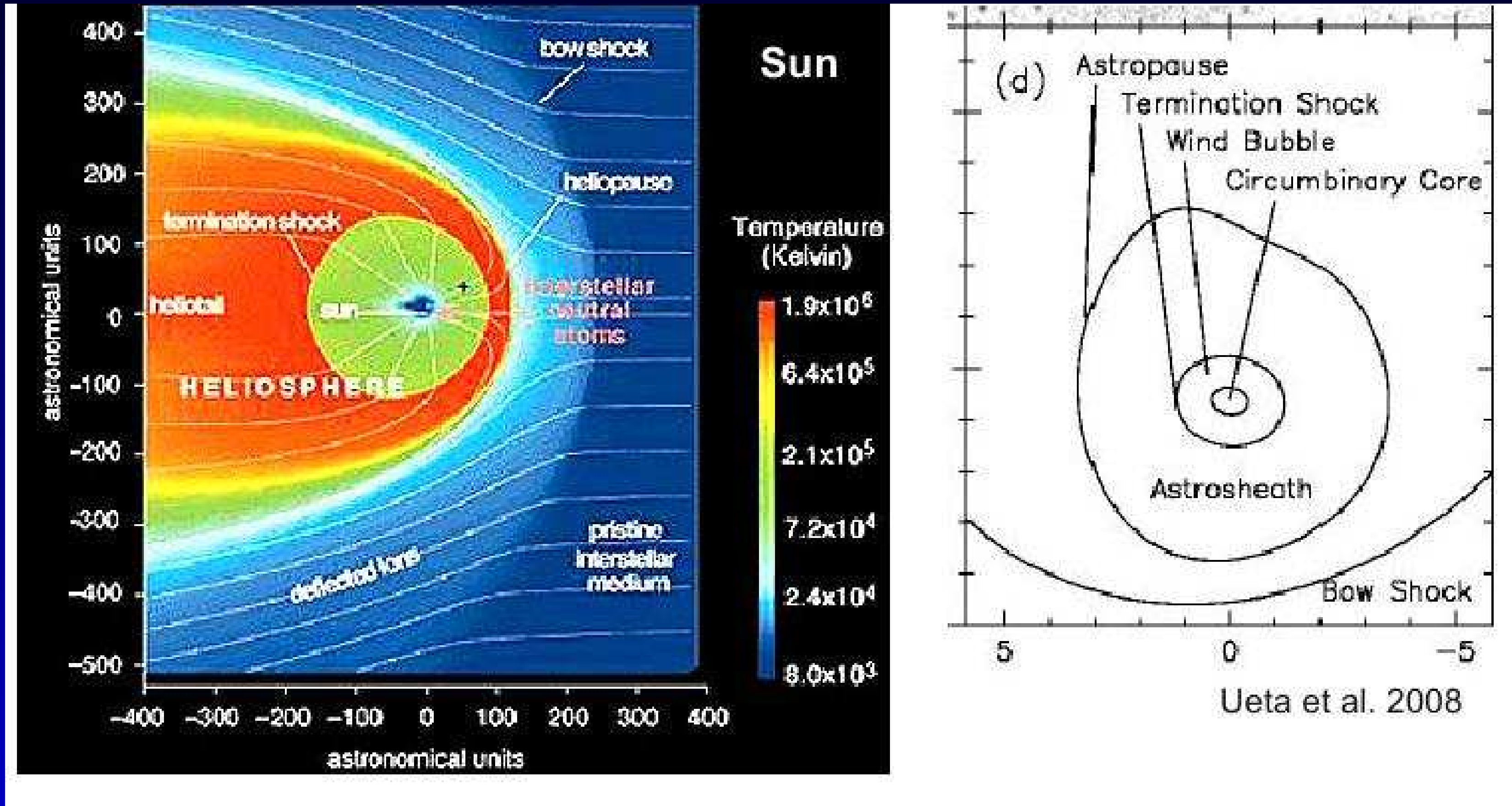

bow shock: where $V_{\rm ISM}$ goes from super- to subsonic
astropause: where $P_{\rm ISM} = P_{\rm CSE}$
termination shock: where $V_{\rm CSE}$ goes from super- to subsonic

Wilkin model

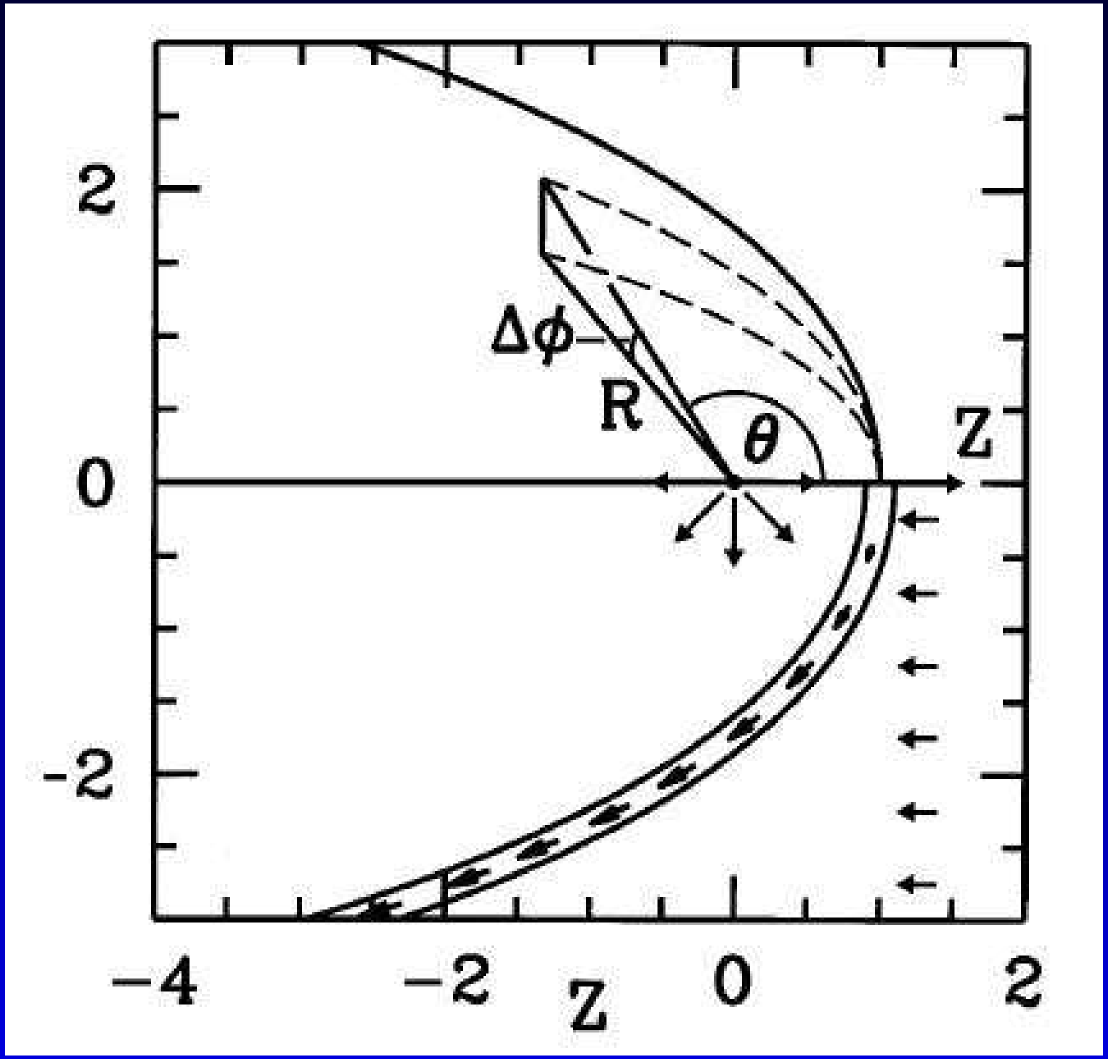

Thin-shell shock model (Wilkin 1996)

Wilkin model

$$R(\theta) = R_0 \sqrt{3 \cdot (1 - \theta / \tan(\theta))} / \sin(\theta)$$

standoff distance:

$$R_0 = \sqrt{(\dot{M}\, V_{\mathrm{exp}}) / (4\pi\, \rho_0\, V_{\mathrm{w}}^2)}$$

3D Wilkinoid

- Monte Carlo simulation
- Fit the outline to an observed profile

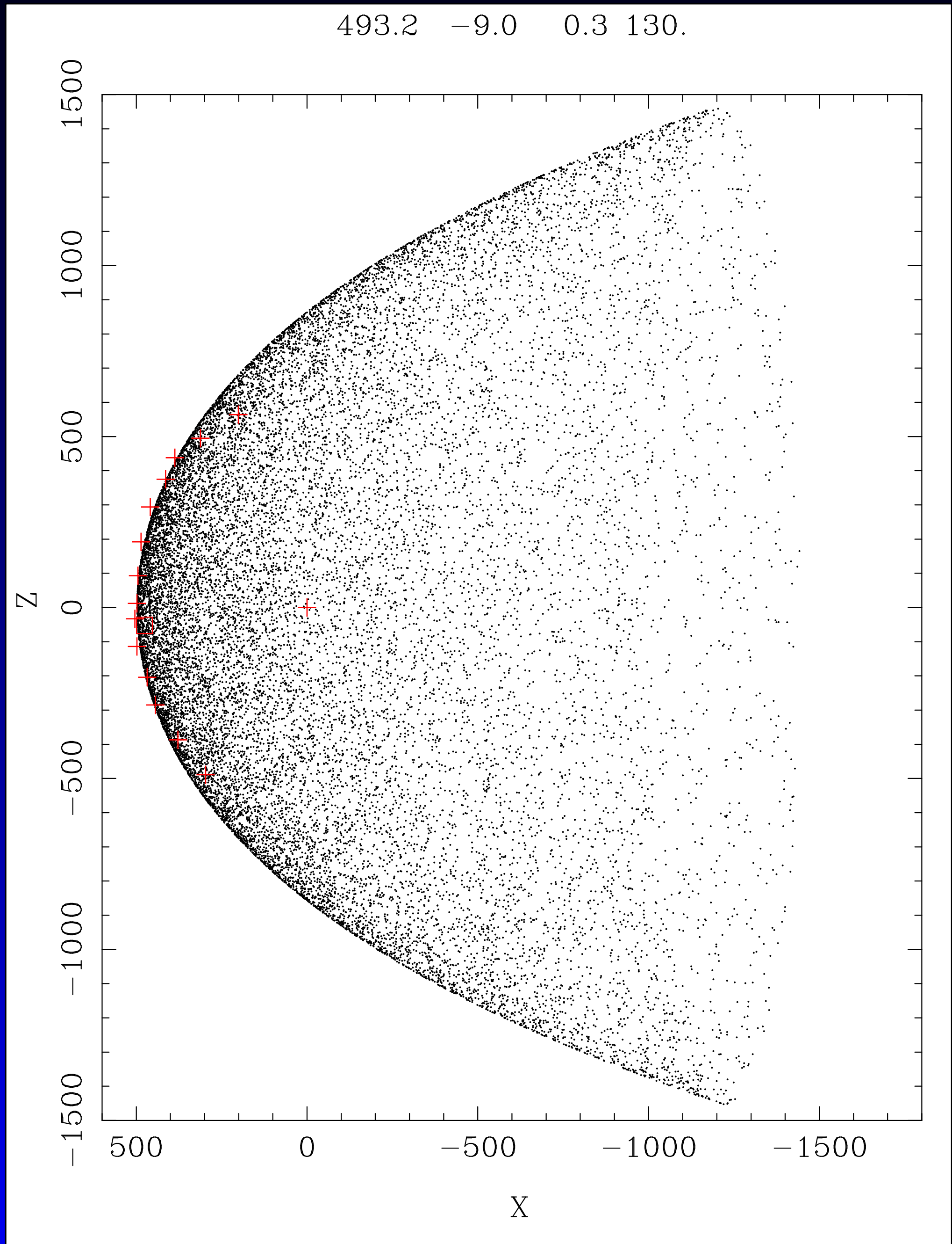
493.2 −9.0 0.3 130.
Z
1500
1000
500
0
−500
−1000
−1500
500
0
−500
−1000
−1500
X

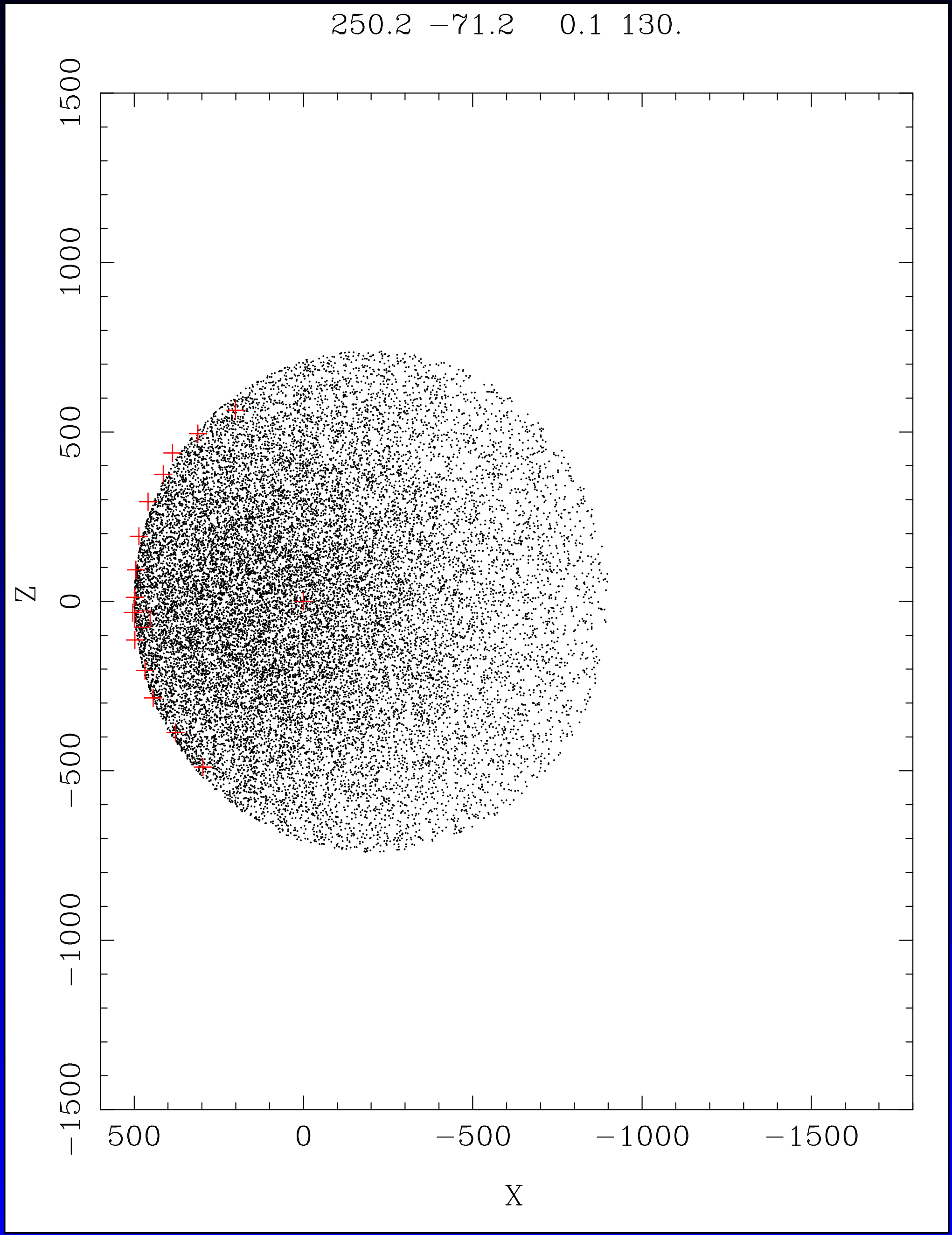
250.2 −71.2 0.1 130.
Z
1500
1000
500
0
−500
−1000
−1500
500
0
−500
−1000
−1500
X

CW Leo - Distance

For any i, predict true distance between bowshock and central star

Radial velocity + proper motions $\Rightarrow i = -33.3 \pm 0.8^\circ$

We assume that the relative peculiar velocity between the ISM and the star is determined entirely by the stars space velocity with respect to the local standard of rest (LSR) In other words, we assume that there is no flow of the ISM itself.

Current best estimate of the distance to CW Leo
$d = 123 \pm 14$ pc; mean $L = 7790 \pm 150\ \mathrm{L}_\odot$

α Ori / Betelgeuse

Decin et al. (2012, A&A 548). ESA press release.

α Ori / Betelgeuse

Only object imaged with multiple arcs

Combines *WISE*, 21 cm GALFA-HI, UV *GALEX*

"Based on the observations and on hydrodynamical simulations, different hypotheses are formulated to explain the origin of the multiple arcs and to understand why no large-scale instabilities are seen in the bow shock region. In our opinion, the two main ingredients to explain both features are (1) a clumpy mass-loss process and (2) the influence of the Galactic magnetic field."

The Zoo

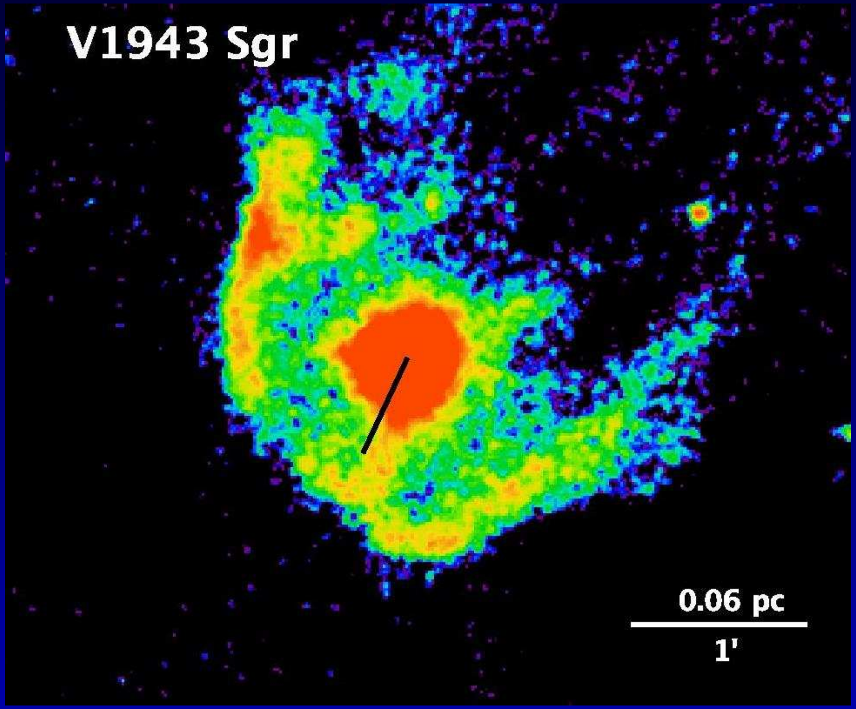

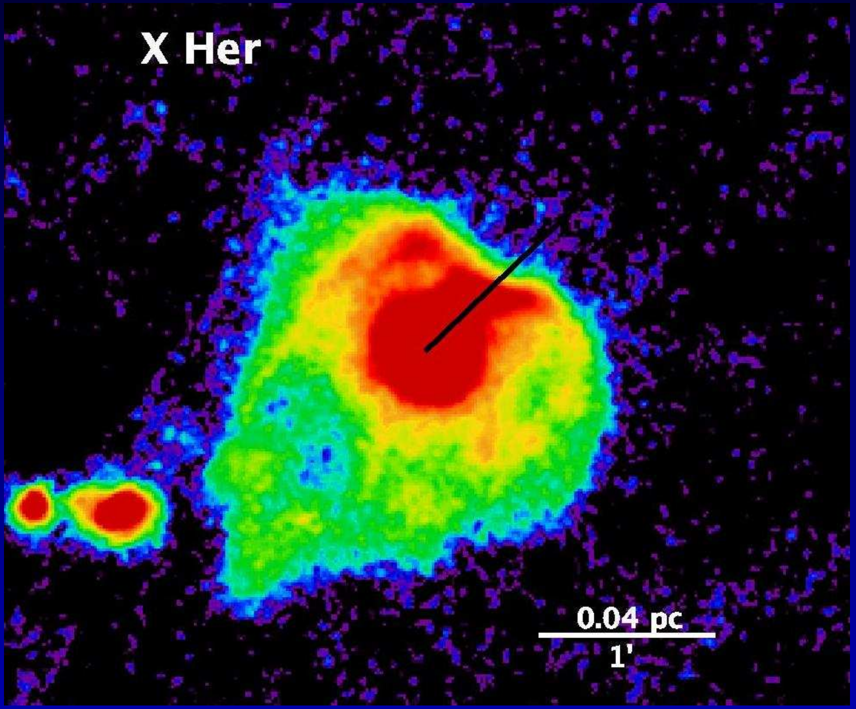

Cox et al. (2012 A&A 537)

"fermata", "eyes", "irregular", and "rings"

stand-off distances, ISM densities

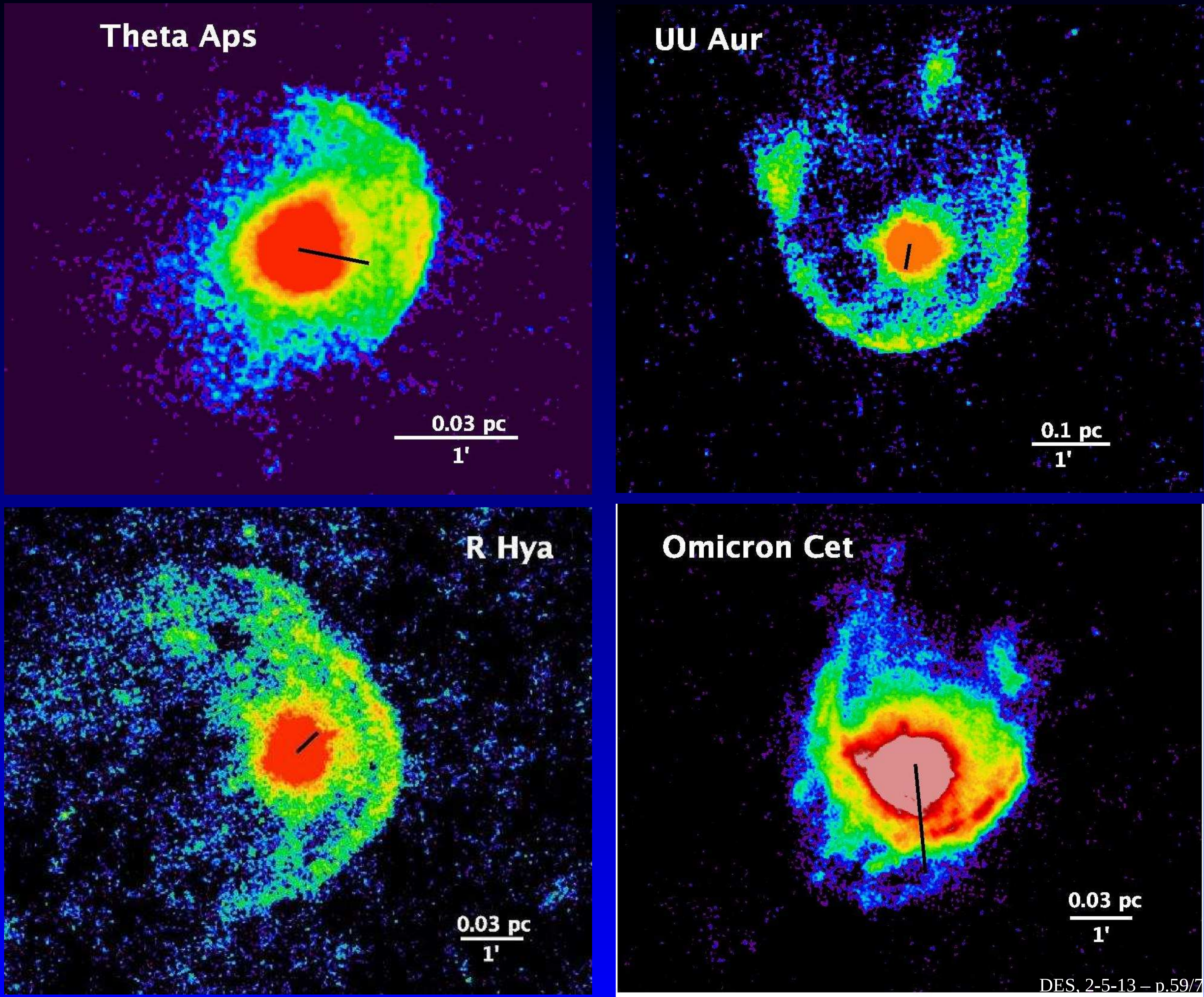
Theta Aps
0.03 pc
1'
UU Aur
0.1 pc
1'
R Hya
0.03 pc
1'
Omicron Cet
0.03 pc
1'

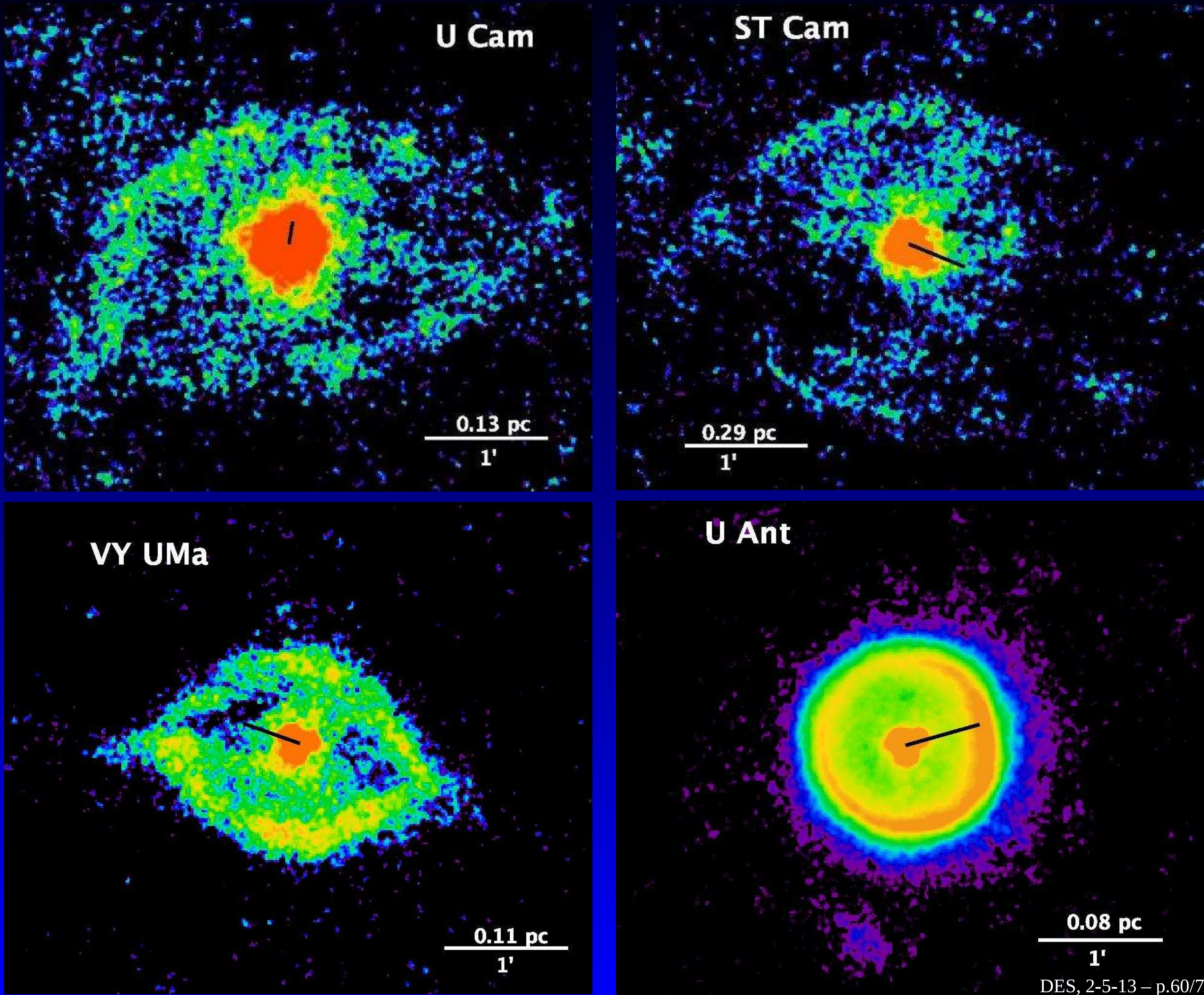
U Cam
0.13 pc
1'
ST Cam
0.29 pc
1'
VY UMa
0.11 pc
1'
U Ant
0.08 pc
1'

Hydro Models

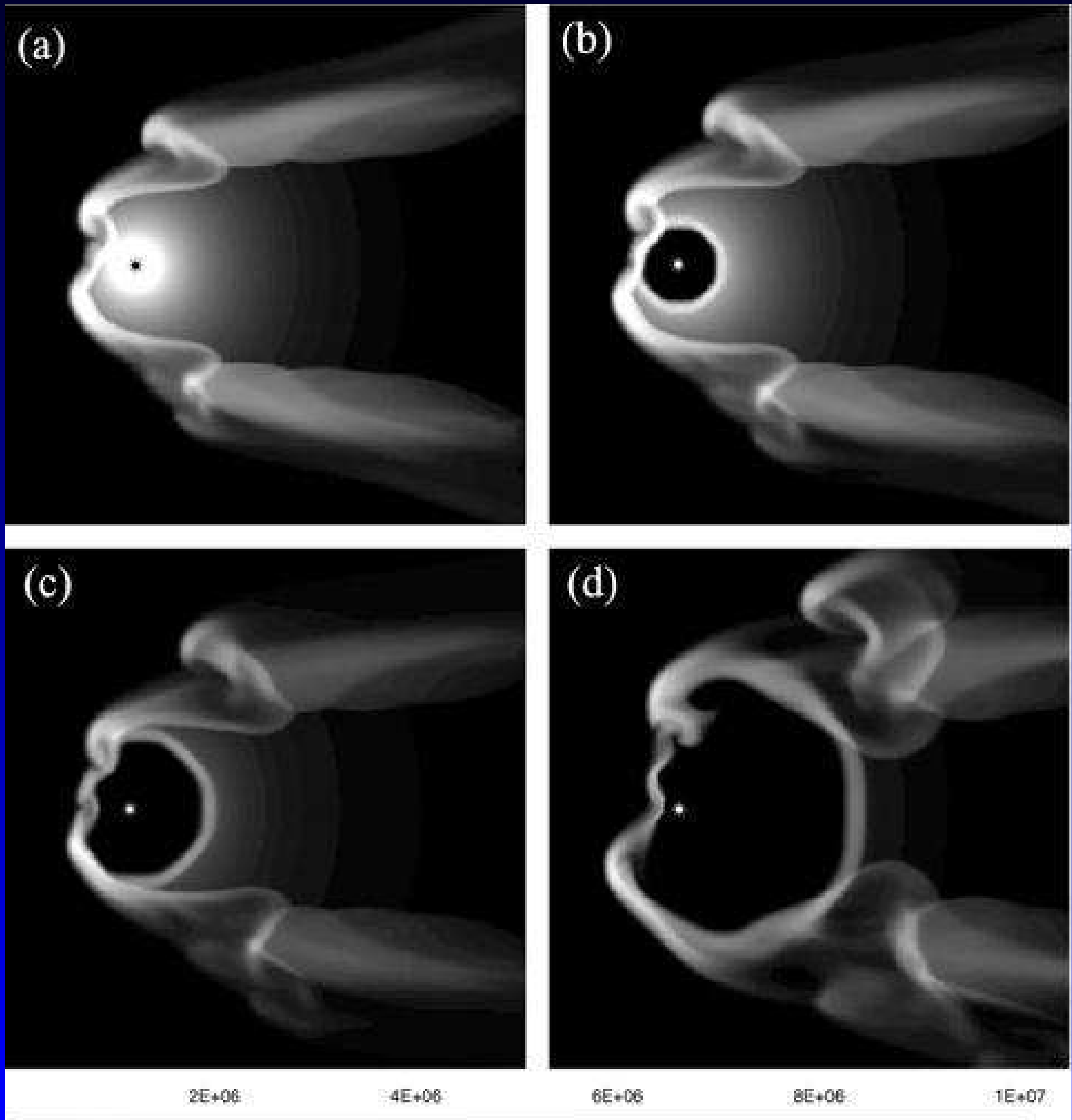

Wareing et al. (2007)

Models

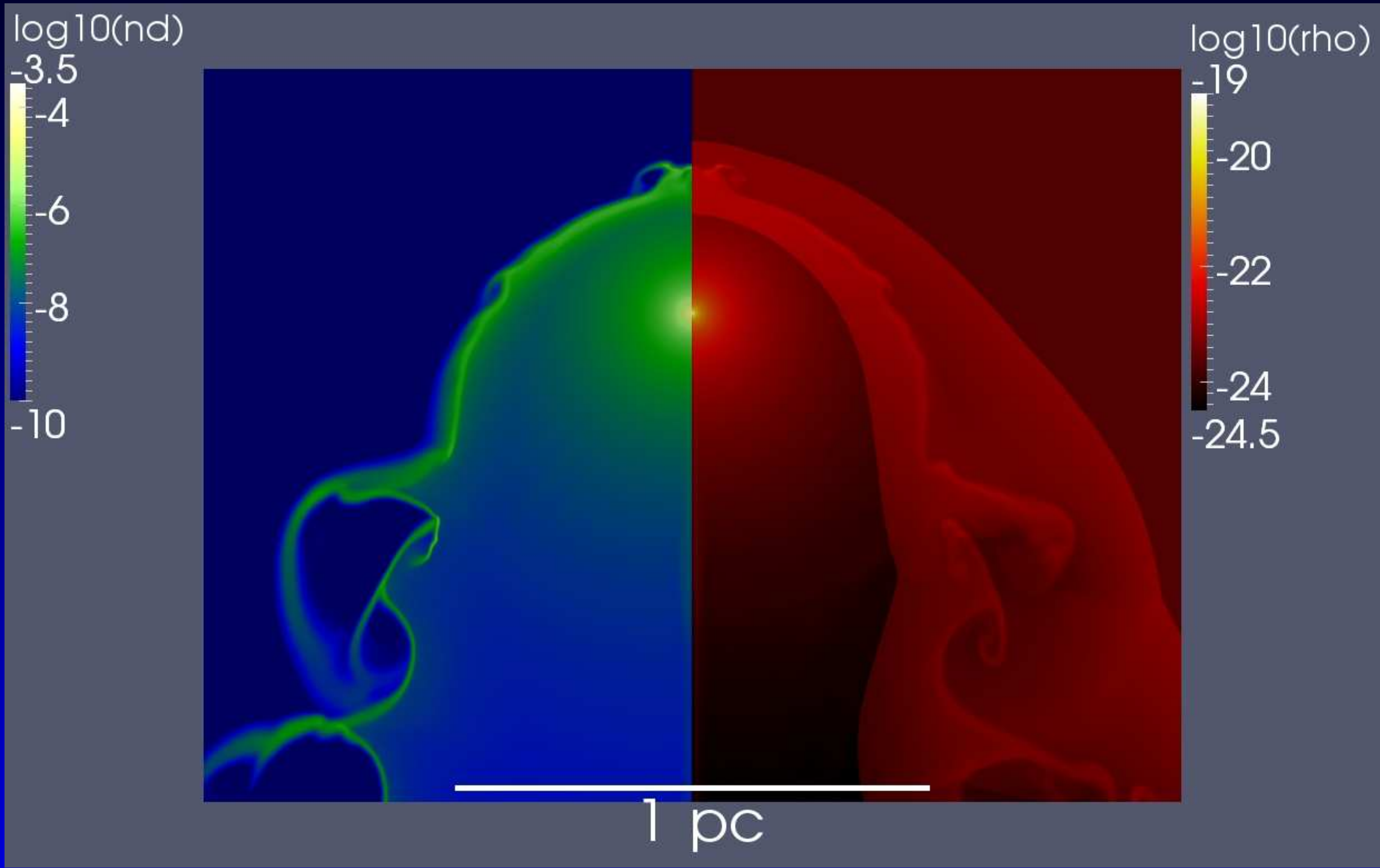

van Arle et al. (2011)

AGB star - Spectroscopy

- CW Leo

-Water
(Decin et al. 2010, Nature)

-HCl lines from J=1-0 up to J=7-6 have been detected.
(Cernicharo et al. 2010, A&A Special Issue)

-Tens of lines from SiS and SiO, including lines from the v=1 vibrational level.
Both species trace the dust formation zone.
(Decin et al. 2010, A&A Special Issue)

AGB star - Spectroscopy

- AFGL 2688, AFGL 618 and NGC 7027
Wesson et al. 2010, A&A special issue

- VY CMa
Royer et al. 2010, A&A special issue

- Dust

CW Leo - Water

Decin et al. 2010, Nature 467, 64

CW Leo - Water

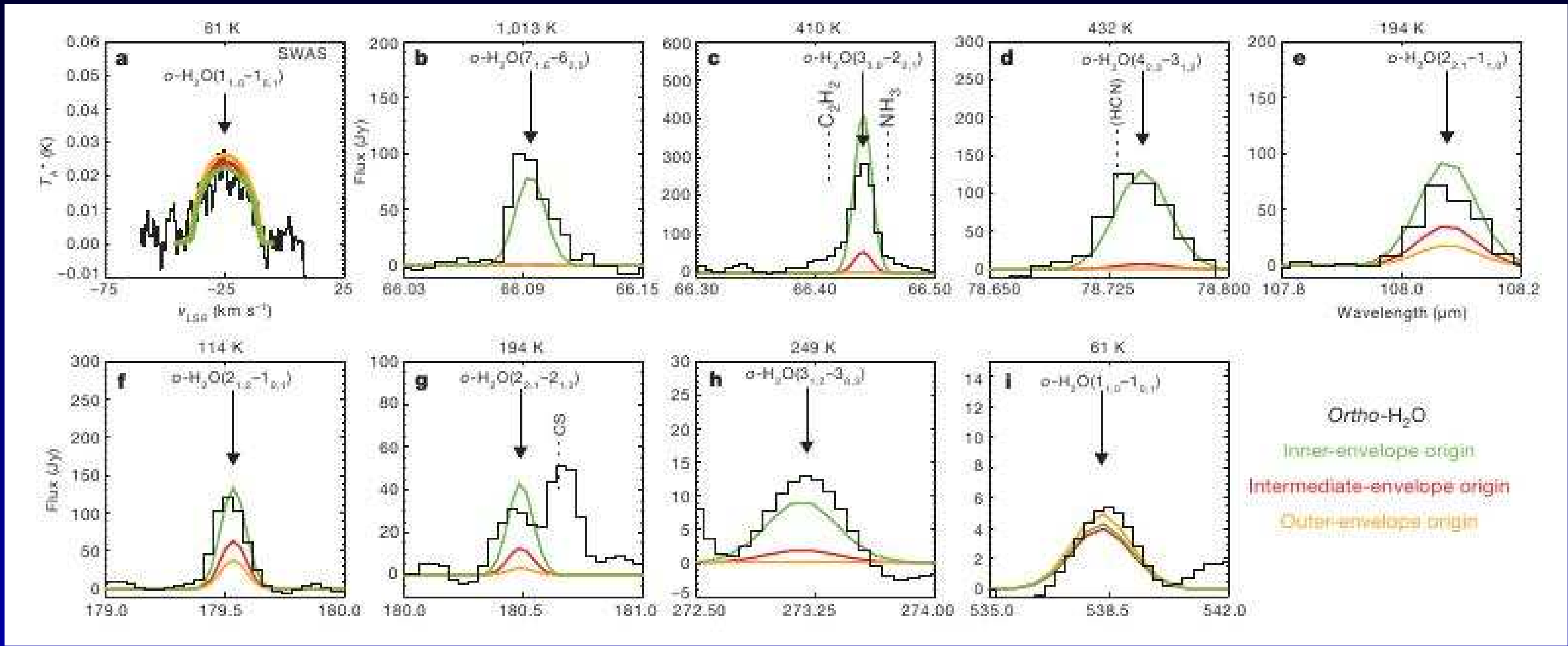

1 line with SWAS

Melnick et al. 2001, Nature 412, 160
"Discovery of water vapour around IRC +10216 as evidence for comets orbiting another star"

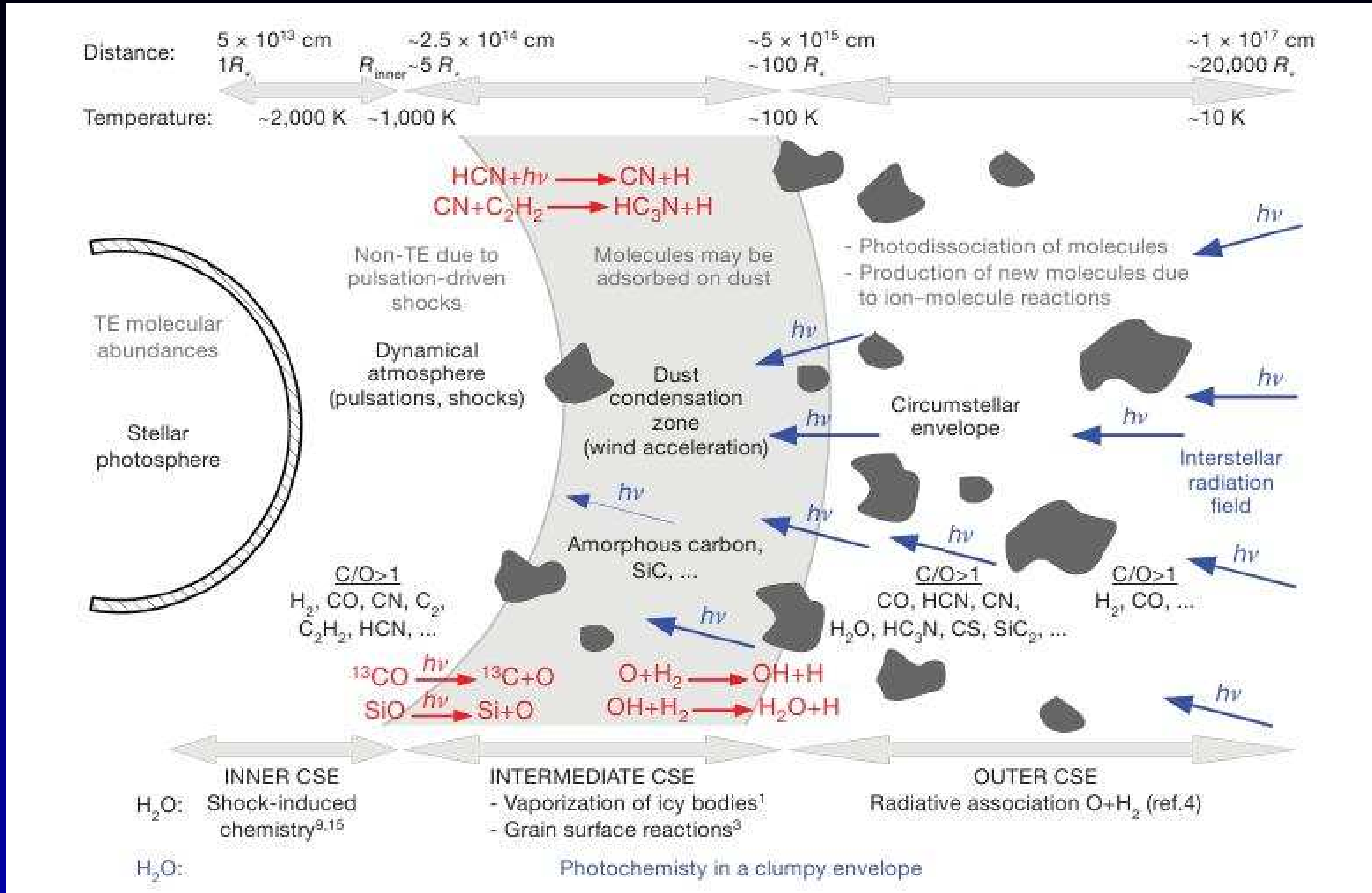

39 ortho-H_2O and 22 para-H_2O with T_{ex} up to 1000 K

"A plausible explanation for the warm water appears to be the penetration of ultraviolet photons deep into a clumpy circumstellar envelope. This mechanism also triggers the formation of other molecules, such as ammonia, whose observed abundances are much higher than hitherto predicted"

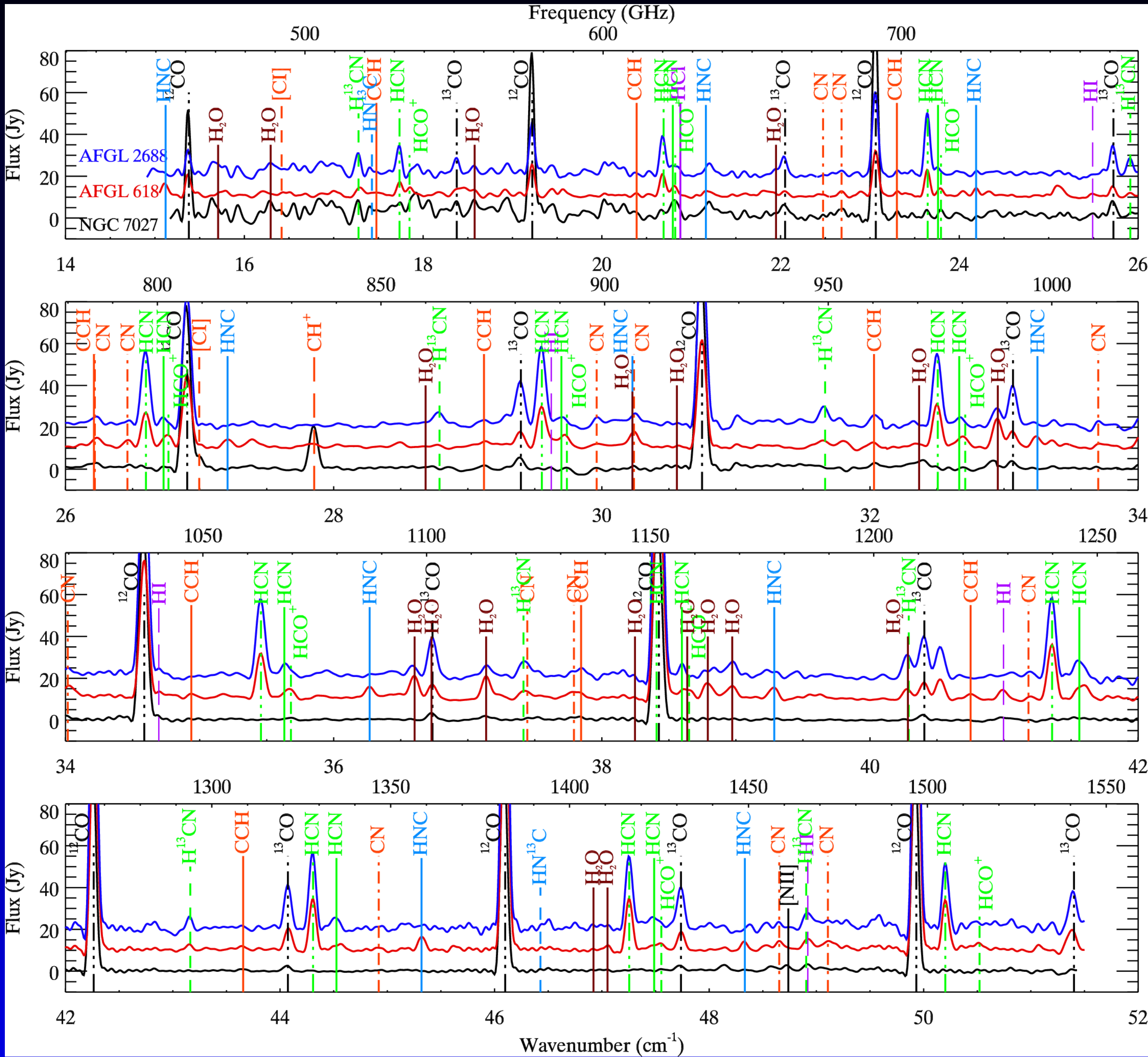

Wesson et al. (2010).

Continuum-subtracted SPIRE FTS spectra of NGC 7027 (black), AFGL 618 (red) and AFGL 2688 (blue)

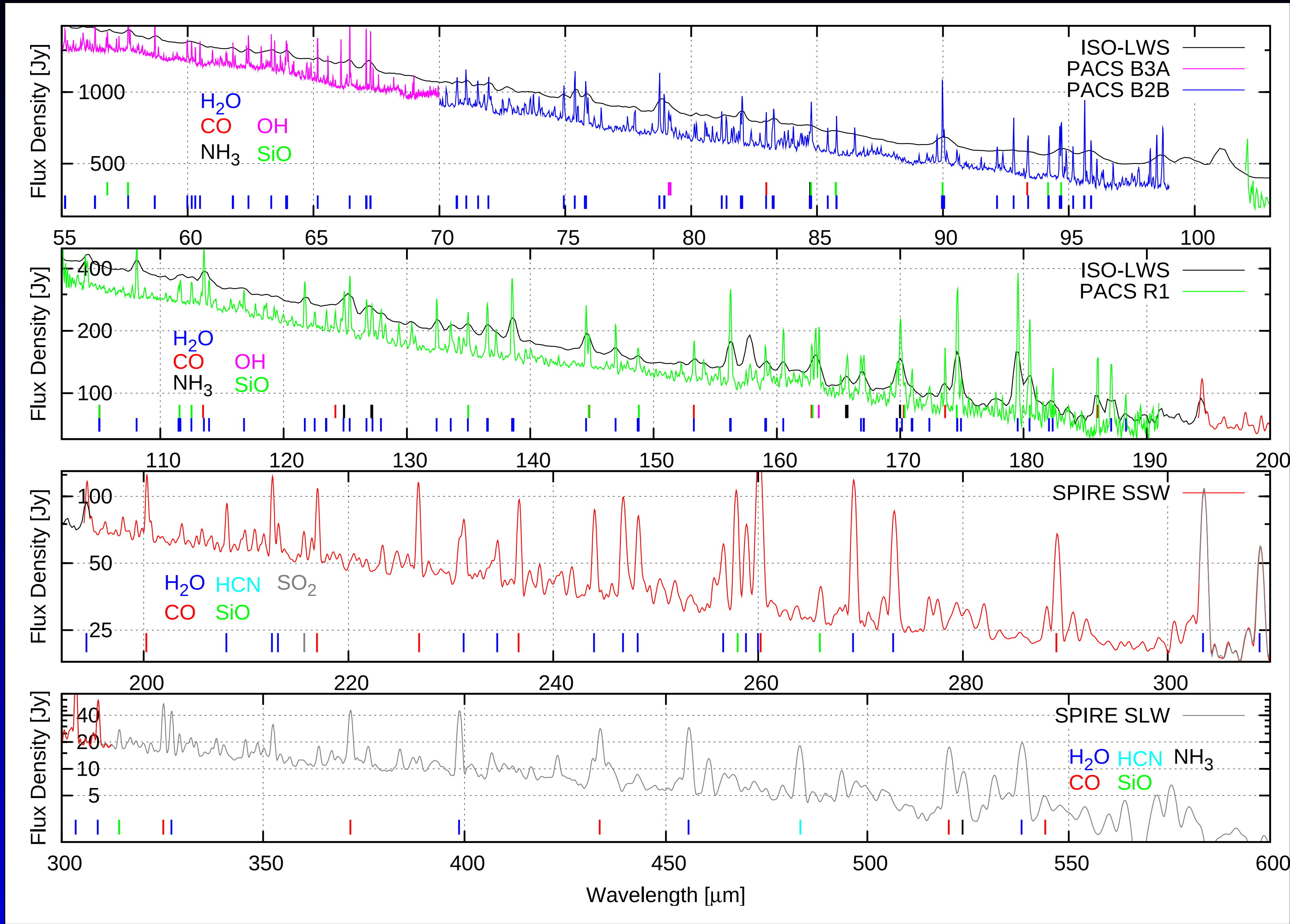

VY CMa, Royer et al. (2010)

Dust spectroscopy

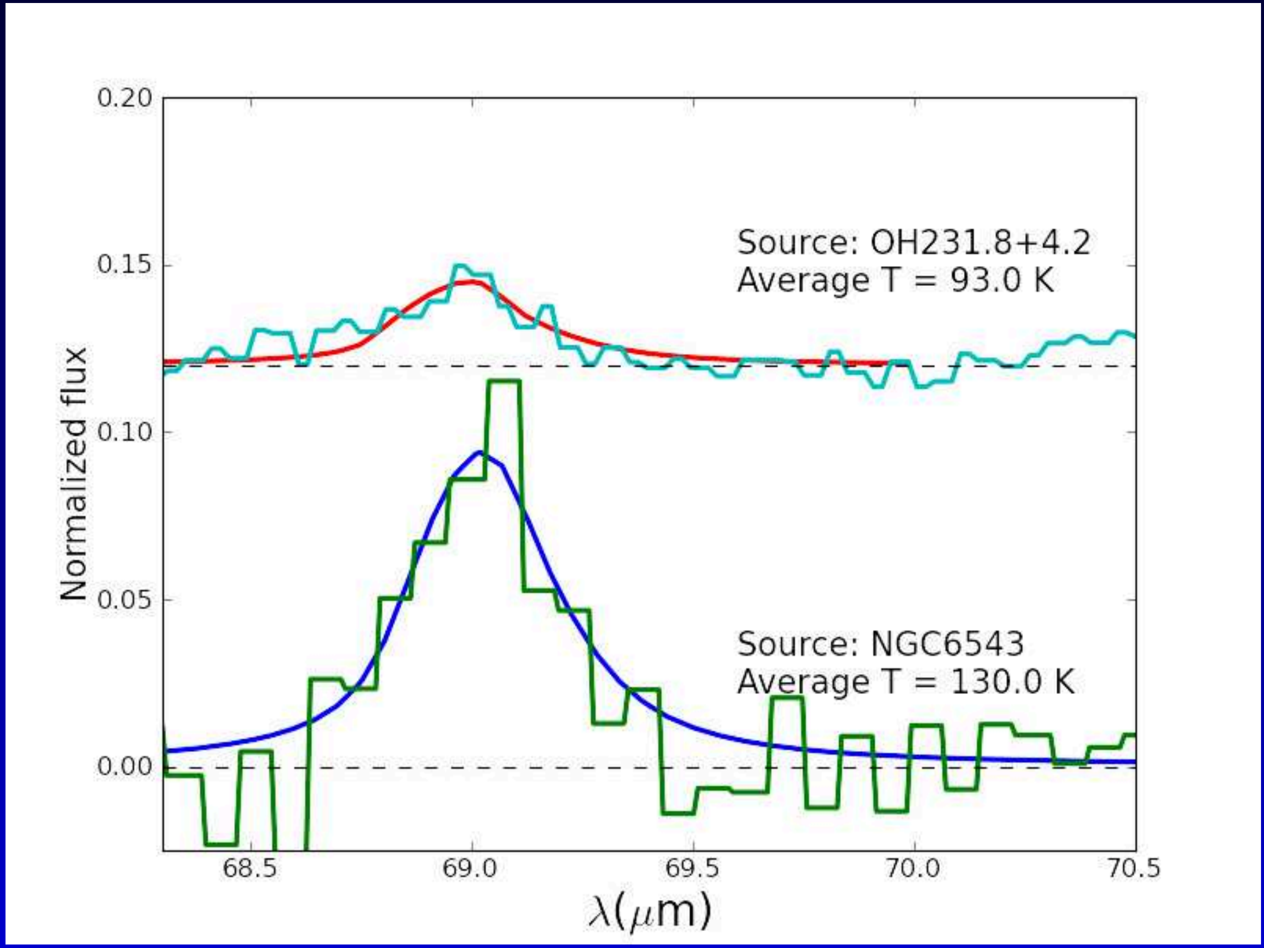

de Vries et al. (2011)

Fosterite at 69μm

Lorentzian fitting - examples

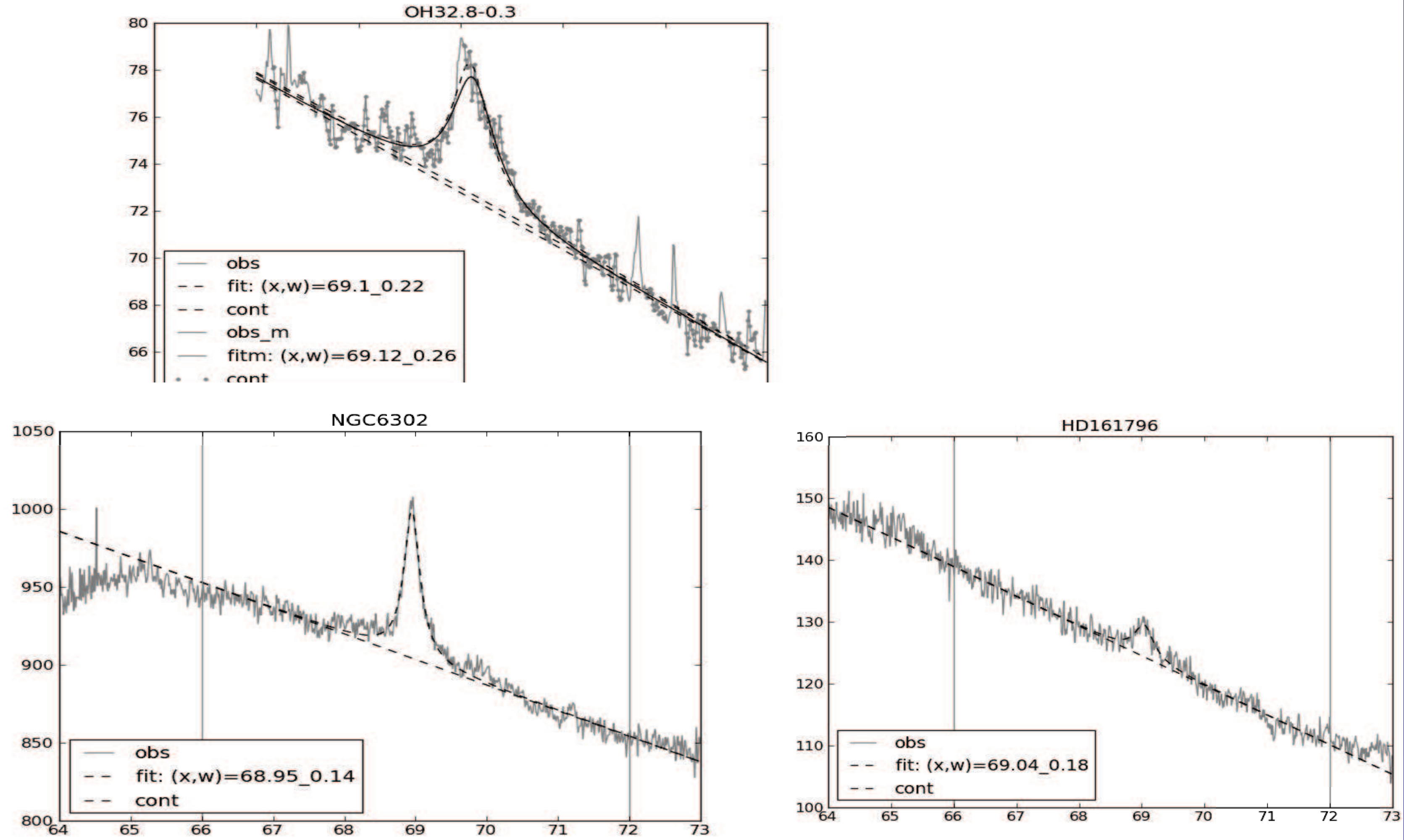

Joris Blommaert et al. (in prep); MESS + GT1 + OT1 (both JB)

14 OH/IR, 14 post-AGB, 10 PNe, 8 Massive evolved stars

Pure Mg-rich for both disk and outflow sources, <200 K.

Conclusions

- Detected ”old” dust mass loss in AGB stars !
- Interaction with the ISM is common
- Influence of binary comparion
- ....and this can happen all at the same time....!
- Line spectroscopy succesfull, and high potential
  - Ongoing improvements in data reduction in spectroscopy ; RSRF; pointing jitter
- Up to the modellers ....
  - Dust + molecules RT modelling ...!!
  - Hydrodynamical simulations ...!!

This MESS is produced by

A. Baier, M. Barlow, B. Baumann, J. Blommaert, J. Bouwman,
P. Cernicharo, L. Decin, L. Dunne, K. Exter,
P. Garcia-Lario, H. Gomez, M.A.T. Groenewegen, P. Hargrave,
Th. Henning, D. Hutsemékers, R. Ivison, A. Jorissen,
F. Kerschbaum, O. Krause, D. Ladjal, T. Lim, M. Mecina,
W. Novotny-Schipper, G. Olofsson, R. Ottensamer,
E. Polehampton, Th. Posch, G. Rauw, P. Royer, B. Sibthorpe,
B. Swinyard, T. Ueta, C. Vamvatira-Nakou, B. Vandenbussche,
G. Van de Steene, S. van Eck, P. van Hoof, H. Van Winckel,
E. Verdugo, C. Waelkens, R. Wesson

FWF-projects: P18939-N16 & I163, P21988
FWO
STFC
ASAP-CO-016/03
PRODEX C90371

THE END